

**DEVELOPMENT OF NEW BIO-FILLER FOR THERMOPLASTIC FROM  
MIMUSOPS ELENGI SEED SHELL POWDER (MESSP)**

**TIFFANY YIT SIEW NG**

**A project report submitted in partial fulfillment of the  
requirements for the award of Bachelor of Engineering  
(Hons.) Petrochemical Engineering**

**Faculty of Engineering and Green Technology  
Universiti Tunku Abdul Rahman**

**September 2016**

## DECLARATION

I hereby declare that this project is based on my original work except for citations and quotations which have been duly acknowledged. I also declare that it has not been previously and concurrently submitted for any degree or award at UTAR or other institutions.

Signature : \_\_\_\_\_

Name : TIFFANY YIT SIEW NG

ID No. : 12AGB06230

Date : \_\_\_\_\_

**APPROVAL FOR SUBMISSION**

I certify that this report entitled **DEVELOPMENT OF NEW BIO-FILLER FOR THERMOPLASTIC FROM MIMUSOPS ELENGI SEED SHELL POWDER (MESSP)** was prepared by **TIFFANY YIT SIEW NG** has met the required standard for submission in partial fulfillment of the requirements for the award of Bachelor of Engineering (Hons.) Petrochemical Engineering at Universiti Tunku Abdul Rahman.

Approved by,

Signature : \_\_\_\_\_

Supervisor : Dr. Mathialagan A/L Muniyadi

Date : \_\_\_\_\_

The copyright of this report belongs to the author under the terms of the copyright Act 1978 as qualified by Intellectual Property Policy of University Tunku Abdul Rahman. Due acknowledgement shall always be made of the use of any material contained in, or derived from, this report.

© 2016, Tiffany Yit Siew Ng. All right reserved.

## ACKNOWLEDGEMENT

I would like to thank everyone who had contributed to the successful completion of this project. I would like to express my gratitude to my research supervisor, Dr. Mathialagan A/L Muniyadi for his invaluable advice, guidance and his enormous patience throughout the completion of the research.

In addition, I would also like to express my gratitude to my loving parents and friends who had helped and given me encouragement. Besides, I would also like to thank the academic staffs of Petrochemical Laboratory, who permitted all the required equipment and knowledgeable guidance to complete the research. Last but not least, I would also like to express my gratitude to my research moderator, Dr. Ong Yit Thai for his considerable help in conducting this research.

## DEVELOPMENT OF NEW BIO-FILLER FOR THERMOPLASTIC FROM MIMUSOPS ELENGI SEED SHELL POWDER (MESSP)

### ABSTRACT

Inadequate recovering, recycling and high consumption of petroleum based polymers such as polypropylene (PP) has greatly increased the global plastic waste. Besides, certain inorganic and organic fillers are incompatible to polymers and may cause restraint in the development and properties of polymer composites. Hence, the usage of natural resources as an alternative of non-renewable materials has been an interesting research to be conducted. In this research, the characteristic and potential of *Mimusops elengi* seed shell powder (MESSP) as filler in PP was studied. MESSP filled PP composites were prepared through melt blending using a Brabender internal mixer at different MESSP loading of 0, 1, 2.5, 5 and 10 wt%. Small particle size, high specific surface area and loose aggregate structure of MESSP in PP attribute to the improved process-ability, tensile modulus, toluene resistance and thermal stability of PP / MESSP composites in comparison to neat PP. However, tensile strength, elongation at break and water resistance of PP / MESSP composites were reduced with increasing MESSP loading. It was studied that the optimum MESSP loading in PP / MESSP composite is in the range of 2.5 - 5 wt% as it showed comparable process-ability and improved elastic modulus, thermal stability and toluene resistance despite of the deterioration occurred in tensile strength, elongation at break and water resistance. SEM morphological observation reveals that the MESSP particles are well dispersed in PP matrix up to 5 wt% which aided on the processing and thermal properties. However, FTIR analysis confirms that there is no chemical interaction between MESSP and PP which is responsible for the low tensile strength, elongation at break and water resistance of PP / MESSP composites as compared to neat PP.

## TABLE OF CONTENT

<b>DECLARATION</b>		<b>ii</b>
<b>APPROVAL FOR SUBMISSION</b>		<b>iii</b>
<b>ACKNOWLEDGEMENT</b>		<b>v</b>
<b>ABSTRACT</b>		<b>vi</b>
<b>TABLE OF CONTENT</b>		<b>vii</b>
<b>LIST OF TABLES</b>		<b>x</b>
<b>LIST OF FIGURES</b>		<b>xi</b>
<b>LIST OF SYMBOLS / ABBREVIATIONS</b>		<b>xiii</b>
<b>LIST OF APPENDICES</b>		<b>xv</b>
 <b>CHAPTER</b>		
<b>1</b>	<b>INTRODUCTION</b>	<b>1</b>
1.1	Background	1
1.2	Problem Statement	3
1.3	Research Objectives	5
 <b>2</b>	 <b>LITERATURE REVIEW</b>	 <b>6</b>
2.1	Thermoplastic	6
2.1.1	Introduction	6
2.1.2	Properties of Thermoplastic Materials	8
2.2	Polypropylene (PP)	10
2.2.1	Introduction	10
2.2.2	Properties of Polypropylene	11
2.2.3	Applications of Polypropylene	13
2.3	Fillers	14

2.3.1	Introduction	14
2.3.2	Natural Fillers / Fibers	16
2.3.3	Advantages and Disadvantages of Natural Fillers / Fibers	18
2.4	<i>Mimusops Elengi</i> Linn	20
2.4.1	Introduction	20
2.4.2	Applications of <i>Mimusops Elengi</i> Linn	21
2.5	Natural Filler Reinforced Polymer Composite	22
2.5.1	Introduction	22
2.5.2	Natural Filler Reinforced Polypropylene (PP) Composite	23
<b>3</b>	<b>MATERIALS AND METHODOLOGY</b>	<b>25</b>
3.1	Introduction	25
3.2	Raw Materials	25
3.2.1	Polypropylene (PP)	25
3.2.2	<i>Mimusops Elengi</i> Seed Shell Powder (MESSP)	26
3.2.3	Miscellaneous Fillers	27
3.3	Preparation of PP / MESSP Composites	27
3.4	Characterization of MESSP and PP / MESSP Composites	29
3.4.1	Particle Size Analysis (PSA)	29
3.4.2	Fourier Transform Infrared Spectroscopy (FTIR)	29
3.4.3	Scanning Electron Microscopy (SEM)	29
3.4.4	Thermogravimetric Analysis (TGA)	30
3.5	Testing of PP / MESSP Composites	30
3.5.1	Differential Scanning Calorimetry (DSC)	30
3.5.2	Swelling Resistance	31
3.5.3	Tensile Test	31



<b>4</b>	<b>RESULTS AND DISCUSSION</b>	<b>32</b>
4.1	Introduction	32
4.2	Characterization of MESSP	32
4.2.1	Particle Size Analysis (PSA)	32
4.2.2	Fourier Transform Infrared Spectroscopy (FTIR)	34
4.2.3	Thermogravimetric Analysis (TGA)	36
4.2.4	Scanning Electron Microscopy (SEM)	38
4.3	Characterization and Testing of PP / MESSP Composites	39
4.3.1	Fourier Transform Infrared Spectroscopy (FTIR)	39
4.3.2	Processing Properties	43
4.3.3	Differential Scanning Calorimetry (DSC)	45
4.3.4	Swelling Test in Water and Toluene	47
4.3.5	Thermogravimetric Analysis (TGA)	49
4.3.6	Tensile Test	51
4.3.7	Scanning Electron Microscopy (SEM)	55
<b>5</b>	<b>CONCLUSION AND RECOMMENDATIONS</b>	<b>59</b>
5.1	Conclusion	59
5.2	Recommendations	60
	<b>REFERENCES</b>	<b>61</b>
	<b>APPENDICES</b>	<b>70</b>

**LIST OF TABLES**

<b>TABLE</b>	<b>TITLE</b>	<b>PAGE</b>
2.1	Properties of Polypropylene	12
2.2	Chemical Families of Fillers for Plastics	15
3.1	Compounding Formulation of PP / MESSP Composites	27
4.1	Physical Properties of MESSP, Carbon Black, Silica and Calcium Carbonate	34
4.2	FTIR Spectroscopy of MESSP	35
4.3	FTIR Analysis of Unfilled PP	40
4.4	FTIR Analysis of PP / MESSP Composites	41
4.5	Data of DSC Analysis of Unfilled PP and PP/ MESSP Composites	47
4.6	TGA Analysis of PP / MESSP Composites at Different MESSP Loading	51
4.7	Tensile Properties of PP / MESSP Composites at Different MESSP Loading	53

**LIST OF FIGURES**

<b>FIGURE</b>	<b>TITLE</b>	<b>PAGE</b>
2.1	Molecular Structure of Thermoplastic	7
2.2	Amorphous and Semi-crystalline Thermoplastic	9
2.3	Chemical Structure of Propylene Repeat Unit	10
2.4	Molecular Structure of Isotactic, Syndiotactic and Atactic Polypropylene	11
2.5	Usage of Polypropylene	13
2.6	Classification of Natural Fibers Based on Their Origins	16
2.7	Structure of Natural Plant Fiber	17
2.8	Flowers and Fruits of <i>Mimusops Elengi</i> Linn	20
2.9	Wood Plastic Composite Bridge for Used by Pedestrians and Golf Carts	23
3.1	Flow Chart of MESSP Preparation	26
3.2	Flow Chart of Preparation and Testing of PP / MESSP Composites	28
4.1	Particle Size Distribution of MESSP	33
4.2	FTIR Spectra of MESSP	36
4.3	TGA Analysis of MESSP	37
4.4	SEM Micrograph of MESSP at 300x Magnification	38

4.5	SEM Micrograph of MESSP at 1000x Magnification	39
4.6	FTIR Spectra of PP / MESSP Composites at Different MESSP Loading	42
4.7	Loading Torque of PP / MESSP Composites at Various MESSP Loading	44
4.8	Stabilization Torque of PP / MESSP Composites at Various MESSP Loading	45
4.9	Water Absorption Percentage of PP / MESSP Composites at Different MESSP Loading	48
4.10	Toluene Absorption Percentage of PP / MESSP Composites at Different MESSP Loading	49
4.11	TGA Analysis of PP / MESSP Composites at Different MESSP Loading	50
4.12	Ultimate Tensile Strength of PP / MESSP Composites at Different MESSP Loading	55
4.13	E-Modulus of PP / MESSP Composites at Different MESSP Loading	54
4.14	Elongation at Break of PP / MESSP Composites at Different MESSP Loading	55
4.15	SEM Micrograph of Tensile Fracture of (a) Unfilled PP, (b) PP / 2.5 wt% MESSP and (c) PP / 10 wt% MESSP at 100x Magnification	56
4.16	SEM Micrograph of Tensile Fracture of (a) PP / 2.5 wt% MESSP and (b) PP / 10 wt% MESSP at 500x Magnification	57
4.17	SEM Micrograph of Tensile Fracture of (a) PP / 1.0 wt% MESSP and (b) PP / 10wt% MESSP at 1000x Magnification	58

**LIST OF SYMBOLS / ABBREVIATIONS**

ABS	Acrylonitrile-butadiene-styrene
Al (OH) <sub>3</sub>	Aluminum hydroxide
Al <sub>2</sub> O <sub>3</sub>	Aluminum oxide
BaSO <sub>4</sub>	Barium sulphate
Bt	Bentonite
CaCO <sub>3</sub>	Calcium carbonate
CaSO <sub>4</sub>	Calcium sulphate
CB	Carbon black
CO <sub>2</sub>	Carbon dioxide
DSC	Differential Scanning Calorimetry
EPDM	Ethylene-Propylene-Diene-Monomer
FTIR	Fourier Transform Infrared Spectroscopy
HIPS	High impact polystyrene
KBr	Potassium bromide
MESSP	<i>Mimusops elengi</i> seed shell powder
Mg (OH) <sub>2</sub>	Magnesium hydroxide
MgO	Magnesium oxide
PC	Polycarbonate
PE	Polyethylene
PP	Polypropylene
PS	Polystyrene
PSA	Particle Size Analysis
PVC	Polyvinyl chloride
Sb <sub>2</sub> O <sub>3</sub>	Antimony trioxide

SEM	Scanning Electron Microscopy
SiO <sub>2</sub>	Silicon dioxide
TGA	Thermogravimetric Analysis
ZnO	Zinc oxide
$\Delta H_m$	Melting heat (J/g)
$\Delta H_{100}$	Melting heat for 100% crystalline polypropylene, 207 J/g
$M_i$	Initial mass of sample before water / toluene immersion
$M_s$	Final mass of sample after water / toluene immersion
$T_c$	Crystallization temperature
$T_g$	Glass transition temperature
$T_m$	Melting temperature
$W_p$	Weight fraction of polymer in sample
wt%	Weight percent
$X_c^m$	Degree of crystallinity

**LIST OF APPENDICES**

<b>APPENDIX</b>	<b>TITLE</b>	<b>PAGE</b>
A	Differential Scanning Calorimetry	70
B	Thermogravimetric Analysis	76

## CHAPTER 1

### INTRODUCTION

#### 1.1 Background

*Mimusops elengi* Linn connects to the *Sapotaceae* family and popularly known as Spanish cherry, Medlar and Bullet wood in English which is a tree primitive to the western peninsular region of South India (Mitra, 1981; Baliga et al., 2011). This plant is a small to large evergreen ornamental tree, growing up to 20 meters in height (Mitra, 1981). As time flies, the tree have disbursed wild in other parts of India, Burma, Pakistan and Thailand (Boonyuen et al., 2009).

In recent decades, there has been much attention on the new demand associated in engineering materials concentrated on its eco-friendliness. Bio-fibers as fillers or reinforcement materials has become a growing trend in polymer composites. The diversity in processing, highly specific stiffness and low economic value of bio-fillers have developed into an attraction to the manufacturers (Faruk et al., 2012). According to PR Newswire, a Compound Annual Growth Rate (CAGR) of 3.9% is expected to increase in the global polymer industry over 2015 – 2020. Polymer is progressively replacing metals, paper, glass and other traditional materials in various applications due to its lightweight, wide range in strength, flexibility in design as well as low cost (Prnewswire.com, 2015). However, a continued rise in the usage of plastic caused the increase in the amount of plastic waste and dependent on fossil fuels (Hamad, Kaseem and Deri, 2013).



Besides, inappropriate disposal of plastic also causes the exposure of pollution effluents and toxic intermediate to the surrounding which can be hazardous (Pollutionissues.com, 2008). Four major ways of plastic disposal is by either landfilling, recycling, incineration or biodegradation and it seems that biodegradation of plastics is the best alternative to decrease the amount of plastic wastes without introducing pollution to environment. The increasing utilization of biodegradable plastic can decrease the carbon footprint, greenhouse gas emissions from polymer consumption and pollution risks (North and Halden, 2013). Thus, bio-fiber or bio-filler reinforced polymer composites with natural organic fillers are getting more acceptance and attention as it improves the biodegradability of polymer by shortening the landfill life spent to be more environmentally friendly and as well as reducing the production cost (Faruk et al., 2012).

With the rising popularity of global resources, the major issues of material availability and environmental sustainability has led to the introduction of natural filler into polymer matrix to produce polymer composites (Faruk et al., 2012). Various research and innovations have been reported in producing thermoplastic based composites by incorporating natural fillers such as kenaf, jute, hemp and cotton into thermoplastic. For instance, kenaf fiber was used as filler in polypropylene (PP) to produce kenaf fiber reinforced PP composites (Shibata, Cao and Fukumoto, 2006).

In this research, *Mimusops elengi* seed shell powder (MESSP) was introduced as a new filler in polypropylene (PP) to form PP / MESSP composites. The main purpose of this research is to determine the potential of MESSP as new bio-filler in PP and to study the effect of MESSP loading on processing, mechanical, thermal and swelling properties of PP / MESSP composites.

## 1.2 Problem Statement

The terms “Renewable energy”, “Sustainable environment” and “Go Green” are among the popular phrase frequently heard these days in many campaigns and environmental related issues. The world from various businesses, organization and agencies, either governmental or private, is trying their best to educate public on the benefits of going green in life (Kuruppallil, Z., 2011). According to Plastics Europe (the Association of Plastics Manufacturers in Europe) (2014), the global production of plastics has escalated gradually more than 60 years from around 0.5 million tons in 1950 to over 299 million tons by the year 2010. Plastics are involved in most aspects of daily life including transportations, packaging materials, telecommunications due to its flexible, durable and lightweight properties (APME, 2007).

However, in conjunction with the increasing plastic production and consumption, its impact to the environment due to increasing plastic waste has become a major issue. Although the amount of petroleum used as the feedstock for plastic manufacturing is less than 5%, the main interest is the sustainability of petroleum as millions of years is required to restore fossil fuels (Kuruppallil, Z., 2011). Besides that, its a big burden to the environment when the harmful chemicals such as benzene and dioxin are released or leached to the environment during the manufacturing or disposal of plastics (Borkowski, 2006).

Most of the plastics products such as containers, cups and bottles are made of petroleum by-products which are non-biodegradable. Thus, it causes the sorting or separation of various types of plastic waste a problematic and labor intensive process, leaving most of the plastic wastes into landfill. Furthermore, most of the plastic materials are contaminated or hard to clean thoroughly for recovering and recycling purpose (Kuruppallil, Z., 2011). Actually, recovering plastic materials from municipal solid waste for recycling or for combustion to generate energy is promising to reduce these issues. Nevertheless, most of the plastic for recycling is shipped to the countries with lower environmental regulations (Gourmelon, 2015). Besides, the cost of recycling of plastic

waste is much higher than it does to produce a new one from scratch which have become a major setback on plastic recycling and recovering (Evans, 2010).

Thus, inorganic fillers such as silica, calcium carbonate ( $\text{CaCO}_3$ ), talc and clay are commonly used in the reinforcement of properties in polymers. The fillers can be varied from low reinforcing clays, alumina trihydrate, silica and other mineral fillers (Mark, 2007). However, these inorganic fillers are incompatible to polymers and may restraint in the development and properties of polymer composites.

In fiber reinforced composites, the main purpose of using carbon fibers is to strengthen the materials by using the strong covalent bonds within the aromatic sheets of the graphite structure. On the contrary, the carbon fibers able to attain only 3 – 4% of the theoretical strength of the aromatic sheets. The carbon fiber structure lack of interconnection between the aromatic sheets, preventing the materials from attaining high strength (Gao, 2004).

Besides that, some other commercially available fillers such as carbon black can be produced by incomplete combustion of hydrocarbons or by thermal cracking (Mark, 2007). It is widely used in strengthening the mechanical properties of polymer and coloring agent in compounding rubber, inks, paints and protective coatings. It had been an effective low cost inert filler in the thermoplastics and elastomers industry. However, there is a sudden increase in the price of carbon black due to its high manufacturing cost, preventing this filler used in high performance application. Thus, manufacturers tends to utilize fillers with lower carbon levels in favor of better performance in the properties of polymer and low cost of final product (Katz and Milewski, 1987).

Due to increased demand on petroleum product, plastic being the major contributor of waste which may cause pollution and not environmentally friendly. Besides, other commercial fillers are either expensive or incompatible, thus usage of organic fillers can help in reducing cost and amount of polymer. However, mainly used organic fillers are

not compatible due to the presence of hydroxyl group. Hence, finding a new filler is a solution for commercial filler in polymer composites.

### 1.3 Research Objectives

The ultimate goal of this research is to characterize and study the potential of MESSP as new bio-filler in PP composite. The other objectives in this research are as followed:-

- (a) To produce and characterize *Mimusops elengi* seed shell powder (MESSP) from *Mimusops elengi* fruit.
- (b) To develop PP / MESSP composite through melt blending method using Brabender Internal Mixer.
- (c) To determine the potential of MESSP as new bio-filler in PP by evaluating the processing, mechanical, thermal properties and chemical stability of PP / MESSP composite as a function of MESSP loading.

## **CHAPTER 2**

### **LITERATURE REVIEW**

#### **2.1 Thermoplastic**

##### **2.1.1 Introduction**

According to Xanthos and Todd (1996), approximately 85% of the polymers produced in the world are thermoplastics and over 70% of the total production of thermoplastic is available in large volume, low cost material resins such as polyethylene (PE), polypropylene (PP), polystyrene (PS) and polyvinyl chloride (PVC). Higher performance and cost of thermoplastics are acrylonitrile-butadiene-styrene (ABS), acrylics and high impact polystyrene (HIPS) (Xanthos and Todd, 1996). In the presence of heat and pressure, waste thermoplastics can be recovered and reprocessabled (Fried, 1995). Thermoplastics can be processed into various shapes through different polymer processing techniques such as extrusion, injection molding, foam molding, thermoforming, rotational molding and calendaring (Craver and Carraher, 2000).

Thermoplastic is a type of polymer by which the backbone of hydrocarbon chains are intermolecularly bonded by van der Waals forces above its transition temperature to form a linear or branched structures. Depending on the arrangement of molecules and the degree of interaction forces between the molecules in the thermoplastic polymer chain, its properties can be varied. Thus, thermoplastic can be differentiated into two natures

relying on the crystallinity in its structure, which is amorphous and crystalline structure (Adhesiveandglue.com, 2016). In addition, thermoplastic is a high molecular weight polymer resulted from a high degree of polymerization. The linear or branched molecular chain does not attached to other polymer chain (NDT Resource Center, 2016). Subsequently, thermoplastic can be repeatedly softened or hardened by increasing or decreasing the processing temperature respectively. This allows the melting of thermoplastic and reprocess into different shapes when heated and become hard and solid upon cooling (Science.jrank.org, 2016). It makes a difference with thermoset, which become irreversibly hard on heating and cannot be recycled (OpenLearn, 2011). Figure 2.1 illustrates the typical molecular structure of a thermoplastic without attaching to other polymer.

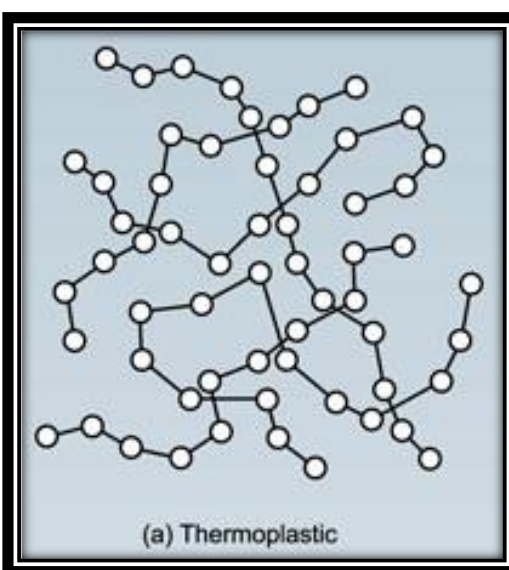


Figure 2.1: Molecular Structure of Thermoplastic (Paroli, Liu and Simmons, 1999)

### 2.1.2 Properties of Thermoplastic Materials

Generally, the polymer chains are randomly arranged and tangled with each other like the threads of a cotton wool pad in an amorphous thermoplastic polymer (Ensinger, 2016). The random molecular orientation directly affects the elasticity of a thermoplastic (Adhesiveandglue.com, 2016). At below glass transition temperature ( $T_g$ ), amorphous thermoplastic is in the state which is known as glassy state, and it possesses the properties of poor resistance to loads and is very brittle. However, there are certain exceptions. For instance, polycarbonate (PC) is highly amorphous thermoplastic but it is tough at below  $T_g$ . This is because it requires huge amount of energy to fracture and behave in a brittle manner. Thus, PC often used as safety helmet and bullet proof glazing due to its excellent impact resistance and dimensional stability (Furness, 2014).

When the temperature is further increased to above glass transition temperature but below melting temperature, amorphous thermoplastic becomes rubbery with excellent elasticity at low loading. It possesses a wide softening range with no distinct melting temperature, moderate heat resistance, low volumetric shrinkage in molding and poor chemical resistance (Adhesiveandglue.com, 2016; BBC, 2014). In addition, when amorphous thermoplastic is heated above the melting temperature ( $T_m$ ), it becomes viscous and possesses viscoelastic behavior (Furness, 2013). When temperature increased, polymer chain gains kinetic energy to move freely and starts to detangle, resulting in low viscosity. Nevertheless, amorphous thermoplastic is able to return to its original position when it is subjected to shear stress within the elastic region (Tver and Bolz, 1984).

On the other hand, semi-crystalline thermoplastics have a highly ordered molecular arrangement with sharp and narrow melting points (Redwood Plastics, 2016). When there is an increment in temperature, it does not soften gradually. It remains as solid until becomes a low viscosity solid upon absorption of certain amount of heat energy. Besides that, semi-crystalline thermoplastic polymer flows anisotropically, shrinking less in the flow direction (RTP Company, 2015). Despite of the orderly polymer structure, the crystalline regions in the polymer chain enhance the strength of thermoplastic, enable it

to withstand high mechanical stresses or loads and better resistance to temperature (Adhesiveandglue.com, 2016). It also exhibits better chemical and fatigue resistance and good for bearing and wear and structural applications (Redwood Plastics, 2016). However, the elasticity of semi-crystalline thermoplastic is not as good as amorphous thermoplastic due to its crystalline region in its structure (Polymer Resources, LTD, 2013).

Figure 2.2 shows the molecular structure of amorphous and semi-crystalline thermoplastic. As shown in the figure, amorphous thermoplastic has random molecular orientation while semi-crystalline thermoplastic has highly ordered arrangement.

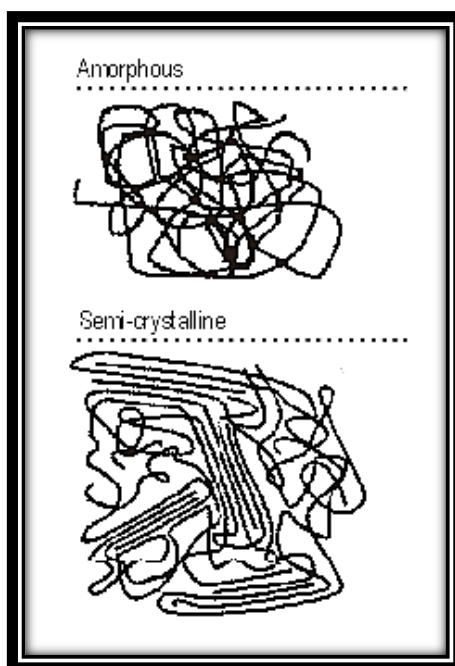


Figure 2.2: Amorphous and Semi-crystalline Thermoplastic (Furness, 2013)



## 2.2 Polypropylene (PP)

### 2.2.1 Introduction

Polypropylene (PP) is among the famous type of thermoplastic material, produced by the polymerization of propylene monomers. In 1954, a German chemist, Karl Rehn and an Italian chemist, Giulio Natta first polymerized propylene to a crystalline isotactic polymer. This important discovery soon led to a larger and commercial production of PP which began three years later (Johnson, 2014). Propylene is a gaseous compound which can be formed by thermal cracking process of petroleum. It belongs to the part of the lower olefins, which contains a single pair carbon atoms linked by a double bond. Thus, the chemical structure of a propylene molecule is  $(\text{CH}_2 = \text{CHCH}_3)$ . Nevertheless, the double bond can be broken and linked thousands of propylene molecules together to form a long polymer chain during polymerization reaction (Raw Items, 2016). Figure 2.3 illustrates the chemical structure of a propylene repeat unit.

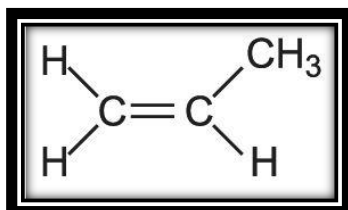


Figure 2.3: Chemical Structure of Propylene Repeat Unit (University of York, 2014)

Propylene molecule is asymmetrical, however when it undergoes polymerization, PP can form three basic of polymeric arrangements, depending on the position of methyl group, which are isotactic, syndiotactic and atactic (University of York, 2014). Figure 2.4 illustrates the molecular structure of isotactic, syndiotactic and atactic polypropylene. As illustrated in Figure 2.4, when PP is arranged in isotactic form, the methyl group has the same orientation at each tertiary carbon atom along the polymer backbone. For syndiotactic orientation, the methyl group alters position on alternative tertiary carbon

atoms. On the other hand, the methyl group places itself randomly on the tertiary carbon atoms in atactic form (Raw Items, 2016).

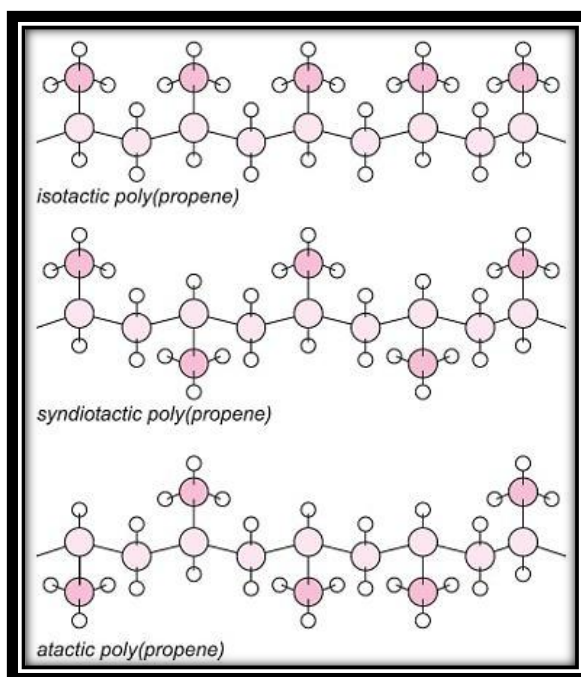


Figure 2.4: Molecular Structure of Isotactic, Syndiotactic and Atactic Polypropylene  
(University of York, 2014)

### 2.2.2 Properties of Polypropylene

Polypropylene fundamentally originate from polyolefin family, thus its properties mainly followed the polyolefin properties. The major properties of PP are semi-rigid, translucent, tough, good chemical resistance, integral hinge property, heat and fatigue resistance (Hindle, 2016).

The arrangement of the methyl group in polypropylene plays an important character to determine the final properties of PP. The polymer chains tend to position themselves in a crystalline structure where the molecules can pack together very closely and stay amorphous in another part of the chain. Thus, PP is a semi-crystalline polymer

which contains crystalline and amorphous region in the molecule. In order to produce a highly crystalline PP, high tacticity of the polymer chain is required. In addition, high rigidity, high strength properties, high heat and chemical resistance also related to the crystallinity of PP. Therefore, the crystallinity of PP highly depending on the size of crystalline region, which is influenced by the nucleation and cooling rate (Raw Items, 2016).

**Table 2.1: Properties of Polypropylene (Textile Technologist, 2012; D&M Plastic Inc., 2016)**

Density	0.905 g / cm <sup>3</sup>
Melting point	170 °C
Glass transition temperature (atactic)	-20 °C (-4 °F)
Glass transition temperature (isotactic)	100 °C (212 °F)
Elongation at break	10 – 45%
Moisture Regain (MR %)	0 %
Elasticity	Very good
Flexibility	Good
Chemical resistance	Excellent
Impact resistance	Excellent
Heat resistance	Moderate
Light resistance	Poor resistance to UV light

### 2.2.3 Applications of Polypropylene

Polypropylene has a wide range of applications which includes consumer products, packaging, laboratory and medical equipment, electric cables, automotive and textiles. In Figure 2.5 illustrates the percentage of usage of polypropylene in our daily life.

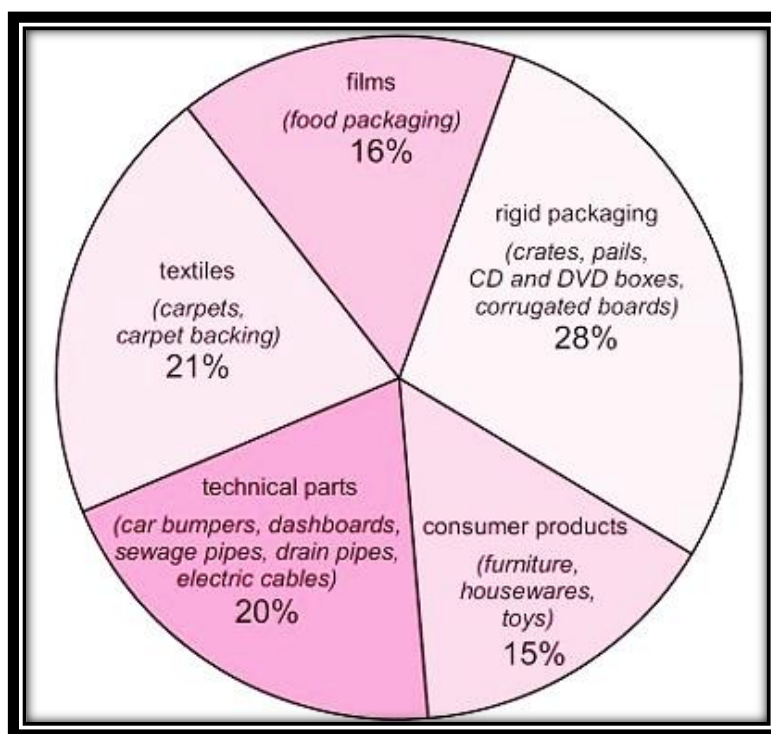


Figure 2.5: Usage of Polypropylene (University of York, 2014)

Polypropylene is well known for its high melting point (approximately 170 °C) and light weight as compared to other polymers, approximately 170 °C. Therefore, PP considered as the optimal choice to hold high temperature of liquids that cool in the bottle. For instance, dishware made of PP will not distort in shape when using hot water in dishwasher whereas dishware made or polyethylene (PE) will be distorted (Raw Items, 2016). This is because polyethylene has a much lower melting point approximately at 100 °C and softens when heated to high temperature (Remichem OÜ, 2016). So, PP is widely used in flexible and rigid packaging application such as yogurt containers, straw,

containers, storage boxes etc. In addition, PP is also used in laboratory and medical equipment due to its moderate heat resistance property.

For automotive industries, PP is popular due to its high chemical and heat resistance, process ability and stiffness. Thus, it is mainly utilized in PP film cushioning, film skins, powder slush molding, bumpers, cladding and exterior trim. Besides that, PP based consumer products such as housewares, furniture, appliances, battery cases toys etc. which is produced by injection molding always appear in life as PP is durable (Hindle, 2016). Apart from that, PP is easy to be modified as it offers an opportunity to add dye to it without changing the quality of polymer. Hence, PP commonly used to make up fibers in carpeting as it strengthens the carpet and make it more durable. It is also found that PP based carpet not only can be used in indoors but also outdoors, where it does not affected by sun, bacteria, mold or other elements (Johnson, 2014).

## **2.3 Fillers**

### **2.3.1 Introduction**

Fillers are particulate materials added to polymers to enhance the physical and chemical properties of polymer and to help to reduce the manufacturing cost of polymer composites. It can be divided according to their origin, function, morphology and composition (Mark, 2007). Most of the fillers are rigid materials, immiscible with the polymer composites in molten and solid states, resulting in the new formation of definite dispersed morphologies. Although certain surface modifiers and processing aids are used at lower amount, fillers can be used at comparatively high concentration (> 5% by volume) (Xanthos, 2010).

Fillers are divided as inorganic and organic substances, then further subdivided based on their origin, shape, size and aspect ratio which shown in Table 2.2 (Xanthos, 2010). According to Wypych in 1999, there are more than 70 kinds of particulates and

more than 15 kinds of natural and synthetic fibers are used as fillers in thermoplastics and thermosets. The most frequently used are industrial minerals such as talc, calcium carbonate, kaolin, aluminum hydroxide, mica, feldspar and wollastonite whereas glass fibers are considered fibrous fillers. In recent times, various natural fillers such as kenaf, jute, wood flour and others are also used in thermoplastics and thermosets composites. Carbon black, considered as a nanofiller and nanoclays such as montmorillonite and hydrotalcite, have been promptly affecting in commercial markets. Besides, graphene sheets are single layers of carbon atoms tightly packed in a honeycomb structure, also functions as one of the most potential fillers in advanced nanocomposites (Jacoby, 2009).

**Table 2.2: Chemical Families of Fillers for Plastics (Xanthos, 2010)**

<b>Chemical Family</b>	<b>Examples</b>
Inorganics	
Oxides	Glass (fibers, spheres, hollow spheres and flakes), MgO, SiO <sub>2</sub> , Sb <sub>2</sub> O <sub>3</sub> , Al <sub>2</sub> O <sub>3</sub> and ZnO
Hydroxides	Al(OH) <sub>3</sub> and Mg(OH) <sub>2</sub>
Salts	CaCO <sub>3</sub> , BaSO <sub>4</sub> , CaSO <sub>4</sub> , phosphates and hydrotalcite
Silicates	Talc, mica, kaolin, wollastonite, montmorillonite, feldspar and asbestos
Metals	Boron and steel
Organics	
Natural polymers	Cellulose fibers, wood flour and fibers, flax, cotton, sisal and starch

### 2.3.2 Natural Fillers / Fibers

Natural fillers are classified based on their origins, either from plants, animals or minerals. Figure 2.6 shows classification of natural fibers based on their origins. As illustrated in Figure 2.6, plant fibers are derived from cellulose such as stalk, root, seed, grass, stem, fruit and leaf whereas animal fibers are derived from proteins such as hair, wool and silk (John and Thomas, 2008).

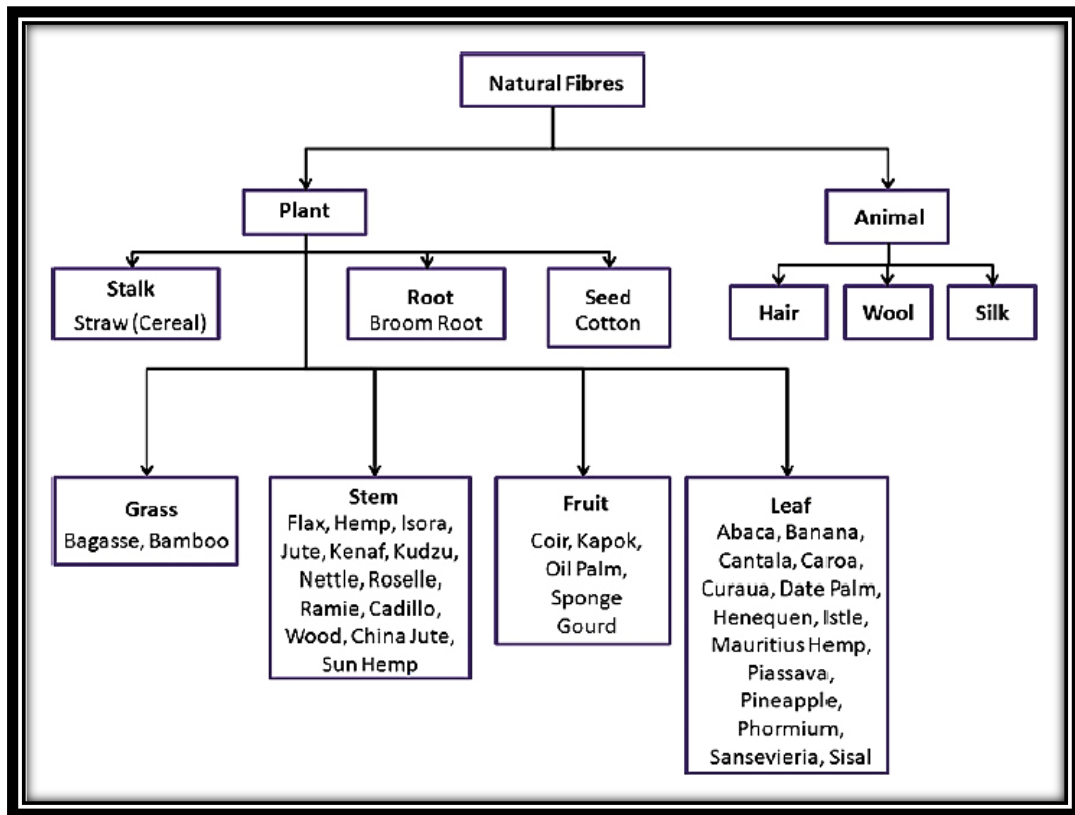


Figure 2.6: Classification of Natural Fibers Based on Their Origins (Azwa et al., 2013)

Natural plant fibers composed of cellulose fibrils attached in lignin matrix. The general structure of a natural plant fiber is illustrated in Figure 2.7. Each fiber consists of a complicated layered structure with a primary cell wall and three secondary cell walls. Among these three secondary cell walls, the mechanical properties of natural filler are determined by the second secondary cell wall. In second secondary cell wall, it contains a

series of helically arranged crystalline cellulose microfibrils formed by long chain of cellulose molecules. Furthermore, there are three main components which are cellulose, hemicelluloses and lignin create each cell wall. Lignin – hemicelluloses acts as mold while microfibrils acts as fibers. Other elements such as pectins and waxy substances also present in the cell wall (John and Thomas, 2008; Dittenber and GangaRao, 2012).

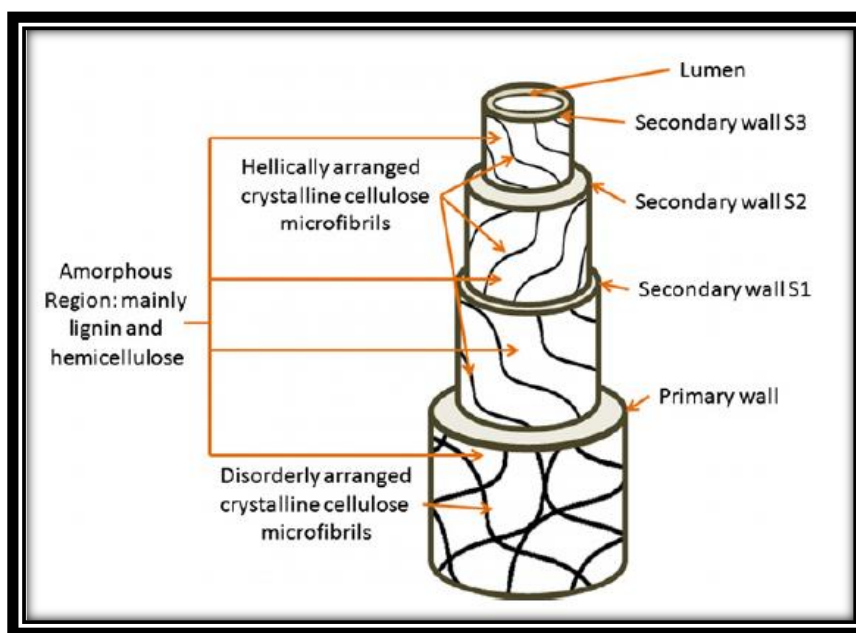


Figure 2.7: Structure of Natural Plant Fiber (John and Thomas, 2008)

Cellulose, a natural polymer, consists of three hydroxyl groups in each repeating unit. It can be found in the slender rod like crystalline microfibrils which arranged along the length of fiber (John and Thomas, 2008). Two of the hydroxyl groups form intramolecular hydrogen bonds within the cellulose macromolecules while other hydroxyl group forms intermolecular hydrogen bond with other molecule (Mwaikambo and Ansell, 2002). Cellulose is relatively strong alkali, hydrolysis and oxidizing agent resistance (John and Thomas, 2008).

Hemicelluloses are lower molecular weight polysaccharides that plays role as supportive matrix for cellulose microfibrils. It is hydrophilic and can be hydrolyzed by acids and alkali. Lignin is a complicated hydrocarbon polymer, providing rigidity to plants



(John and Thomas, 2008). It is hydrophobic in nature and resistance to acid hydrolysis, but soluble in hot alkali, readily oxidized and easily condensable with phenol (Mohanty, Misra and Drzal, 2005). Pectin is a collective name for heteropolysaccharides which contributes in the flexibility of plants. Waxes contain various types of alcohol and protect fiber (John and Thomas, 2008; Wong, Yousif and Low, 2010).

### **2.3.3 Advantages and Disadvantages of Natural Fillers / Fibers**

Recently, many researches and scientists has pay attention to natural fillers and fibers as a substitute of commercial fillers in polymer composites due to their benefits over conventional glass and carbon fibers. The natural fillers include jute, kenaf, flax, hemp, bagasse and many others. Generally, natural fillers can lower the production and manufacturing cost with the requirement of lower specific weight by comparing with glass reinforced composites, resulting in higher specific strength and stiffness for polymer composites. They are safer to approach in working area compared to synthetic reinforced polymer fiber (John and Thomas, 2008).

Besides that, natural fillers can be recycled and also labelled as a renewable source which do not involve in the carbon footprint. Excess carbon dioxide does not circulate into the atmosphere when natural fillers undergo combustion, resulting in very low energy requirement in production. Consequently, natural fillers provide a more environmental friendly atmosphere and reduce dermal and respiratory irritation. In addition, natural fillers can act as a good electrical insulator as its hollow cellular structure equips with good acoustic insulating properties fiber (John and Thomas, 2008).

The structure of natural filler can be differentiated through crystalline and amorphous region. Large amount of strong intramolecular hydrogen bonds formed resulting in the formation of cellulose block and chemicals face difficulty in penetration. However, the hydrophilic hydroxyl groups exist in the amorphous region form hydrogen

bonds with water molecules from the atmosphere, causing dyes and resins to be absorbed easily in this region (Kabir et al., 2012). This situation causes a major drawback to natural filler reinforced composite due to the polar and hydrophilic nature of natural filler and the non-polar nature of thermoplastics, developing problems in compounding and non-uniform dispersion of fillers within the matrix which decreases the efficiency of the polymer composite (John and Thomas, 2008).

According to Joseph et al. in 2003, natural filler starts to degrade at 240 °C. The main components in filler which are cellulose, hemicellulose and lignin are sensitive to different range of high temperatures. It becomes a disadvantage in the choice of matrix material when the processing temperature of polymer composites has to be restricted to 200 °C as lignin undergoes degradation at higher temperature.

As mentioned above, hydrophilic and moisture absorption characteristic of natural filler results in formation of new hydrogen bonds with water molecule from the atmosphere. The cross section of the natural filler becomes the main entry of water penetration. When the hydrophilic natural filler mixed with hydrophobic thermoplastic, fillers will absorb and swell in the matrix. This causes a setback as the bonding strength at the interface is weakened, in consequence to instability of dimension, cracking of matrix and poor mechanical properties of polymer composites (Zakaria and Kok Poh, 2002). In addition, air molecules may be trapped inside the polymer composite when the natural filler is introduced into the matrix. Presence of voids will be formed in the crystalline and amorphous region of the matrix. This condition gives an effect of sudden failure and poor mechanical properties of polymer composite (Kabir et al., 2012).

## 2.4 *Mimusops Elengi* Linn

### 2.4.1 Introduction

Natural resources especially plants have been acting an essential role in traditional medicine for thousands of years (Kadam et al., 2012). One of the famous traditional medicinal plant is known as *Mimusops elengi* Linn, which generally also known as Bakul and Spanish cherry, connecting to *Sapotaceae* family (Mitra, 1981; Baliga et al., 2011). It is a small to large ornamental evergreen tree found in India, Burma, Pakistan and Thailand (Boonyuen et al., 2009).

*Mimusops elengi* grows with dark grey bark, covered with vertical lenticels, cracks and longitudinal fissures (Dymock, 1890). The leaves are glossy and are in dark green when old. The new leaves usually appear in February. Flowers are white and fragrant. Fruition happens in rainy season (Kadam et al., 2012). The berry is smooth and in yellow when ripe and edible while the seed is grayish brown (Dymock, 1890). Stem bark, flowers, leaves, fruits and seeds are usually used in daily life (Raghunathan and Mitra, 2000).



Figure 2.8: Flowers and Fruits of *Mimusops Elengi* Linn (Lalithamba, 2011)

### 2.4.2 Applications of *Mimusops Elengi* Linn

In traditional medicinal industry, the bark of *Mimusops elengi* can be used as a coolant or cardio tonic to cure stomatitis and helps to strengthen gums and teeth (Rajkumara, Pandiselvi and Sandhiya, 2012). Its soup is also helps to recover from fever and body ache. Its leaves can be utilized to cure leucorrhoea, excessive sweating and hemorrhage. Besides, the flowers can be used to treat running nose, headache and liver complaints. Since the flowers are fragrant, it can also be used to manufacture perfume. Due to its astringent property, the fruit of *Mimusops elengi* can be used to cure diarrhea and chronic dysentery (Roqaiya et al., 2015). According to Kadam et al., the seed can be used to fix headache and strengthens teeth.

Since the seed from *Mimusops elengi* can be used as traditional medicine, there are some researchers have been investigating the composition of fatty acid contained in the seed. Based on the research done by Dutta and Deka (2014), high content of fatty acid such as palmitic acid (53.55%), oleic acid (28.52%), followed by stearic acid (10.26%) and linoleic acid (7.65%) were detected in *Mimusops elengi* seed oil. This proves that abundant amount of fatty acid methyl ester (FAME) indicates the formation of biodiesel, becoming an alternate renewable and biodegradable fuel in our daily life (Deepanraj et al., 2015).

## 2.5 Natural Filler Reinforced Polymer Composite

### 2.5.1 Introduction

Natural filler acts as reinforcement of polymer matrix has becoming an attractive research over the past decades. Natural filler reinforced polymer products had been earning importance in different industrial applications such as automotive, packaging, furniture and building and construction. This polymer composite became a highly potential material to replace steel, concrete, glass fiber and wood which mainly used in construction applications (Pickering, 2008).

Pujari et al. stated that there are some natural fillers such as rice husks, flax, hemp and jute fibers in both structural and non-structural usage. Due to environmental concerns and the crude oil reserves, the application of natural fillers in polymer composite production will offer great advantages to environmental and cost in a competitive market. Therefore, natural filler reinforced polymer composite products are important and have been utilized in different industrial applications due to it's:-

- Better flexibility in complex shape and design
- Less abrasive than glass fibers
- Better mechanical properties
- Lower manufacturing cost compared to mineral and glass fiber filler
- Better acoustic and thermal insulation properties
- Can be recycled as it is biodegradable
- Carbon dioxide (CO<sub>2</sub>) and greenhouse gases emission can be reduced
- Conservation of oil and gas resources (Pickering, 2008)

### 2.5.2 Natural Filler Reinforced Polypropylene (PP) Composite

According to research, timber products manufacturer foreseen plastics to play an important role in construction materials, which possesses some characteristics that timber does not have, including moisture and insect resistance. In addition, wood is a resource that readily available, relatively low cost filler that can reduce the cost of raw materials in polymer processing, enhance the stiffness of polymer and increase the extrusion rate of extrudate profiles as the cooling rate of wood is higher than plastics (Thomas and Pothan, 2009). Wood flour has become one of the natural fillers in polymer composite material due to its low maintenance, lower impact on the environment and high strength and stiffness. For instance, a pedestrian bridge was installed for use by golf carts in Guelph, Ontario early in 2007 as illustrated in Figure 2.8. The bridge was made with 30% wood fiber / oriented polypropylene (PP) and has a density of  $0.55 \text{ g / cm}^3$  (Pritchard, 2007).



Figure 2.9: Wood Plastic Composite Bridge for Used by Pedestrians and Golf Carts  
(Pritchard, 2007)

In year 2000, Toyota Boshoku succeeded in commercializing a kenaf base material which contain kenaf and PP resin to use as door trim. Kenaf is a plant that can be found in tropical and semi-tropical regions and it is harvested for its bast fibers. There are few attractions possessed by kenaf fiber are relatively inexpensive, low density of  $1.40 \text{ g / cm}^3$

compared to glass  $2.2 \text{ g / cm}^3$  and high mechanical properties (Faruk et al., 2012). One of the characteristics of kenaf which is high fiber strength assists to decrease weight while maintains the same durability level as conventional products (Toyota Boshoku, 2016).

Besides that, jute is one of the lowest cost natural fibers and has the highest production volume of bast fibers. It can be found anywhere in Bangladesh, India and China. Jute plants require very low amounts of fertilizer and pesticides and help to cleanse the air by consuming large volume of carbon dioxide (Rashid, 2010). Jute reinforced PP composite mainly used in automobile industries, including door panels, seat backs, headliners, dash boards and trunk liners. This is because jute fiber is lighter in weight and has better serviceable physical and mechanical properties. When jute reinforces with PP matrix, the polymer composite possesses few properties such as fire, termite and better moisture resistance, available at semi-finished or finished state to reduce labor and finishing cost and the most essential advantage is it can be recycled (Das, 2009).

However, natural fillers are not totally free from problems and they have significant disadvantages in their characteristics. Mohammed et al. (2015) stated the hydrophilic characteristic of natural fibers allows moisture absorption from the surroundings which leads to weak interaction between the fiber and polymer. Moreover, waxy fiber surfaces and other non-cellulosic substances also form poor adhesion between fiber and PP matrix, subsequently resulting in poor tensile properties of natural filler reinforced PP composites (Ku et al., 2011).

## **CHAPTER 3**

### **MATERIALS AND METHODOLOGY**

#### **3.1 Introduction**

This chapter includes the details of raw materials being used for the preparation of PP / MESSP composite, the sources of materials and the composite preparation method specified with the parameters. Lastly, the characterizations and composite testing methods are also specified in this chapter.

#### **3.2 Raw Materials**

##### **3.2.1 Polypropylene (PP)**

The PP resins used to prepare PP / MESSP composites were supplied by Lotte Chemical Titan (M) Sdn. Bhd.



### 3.2.2 *Mimusops Elengi* Seed Shell Powder (MESSP)

The *Mimusops elengi* seed shell used to convert into powder was obtained from ripe fruits of *Mimusops elengi* plant at around Taman Kampar Perdana, located in Kampar, Perak, Malaysia. The seed shell was dried under the sunlight for 4 – 5 hours for a period of one week and cleaned with distilled water at 80 °C for 2 hours. The clean seed shell was then dried in a vacuum oven at 80 °C for 24 hours, crushed and grinded to obtain in powder form. The powder was then sieved to obtain an average particle size of below 45 µm. The preparation procedure of MESSP from *Mimusops elengi* fruit is shown in Figure 3.1.

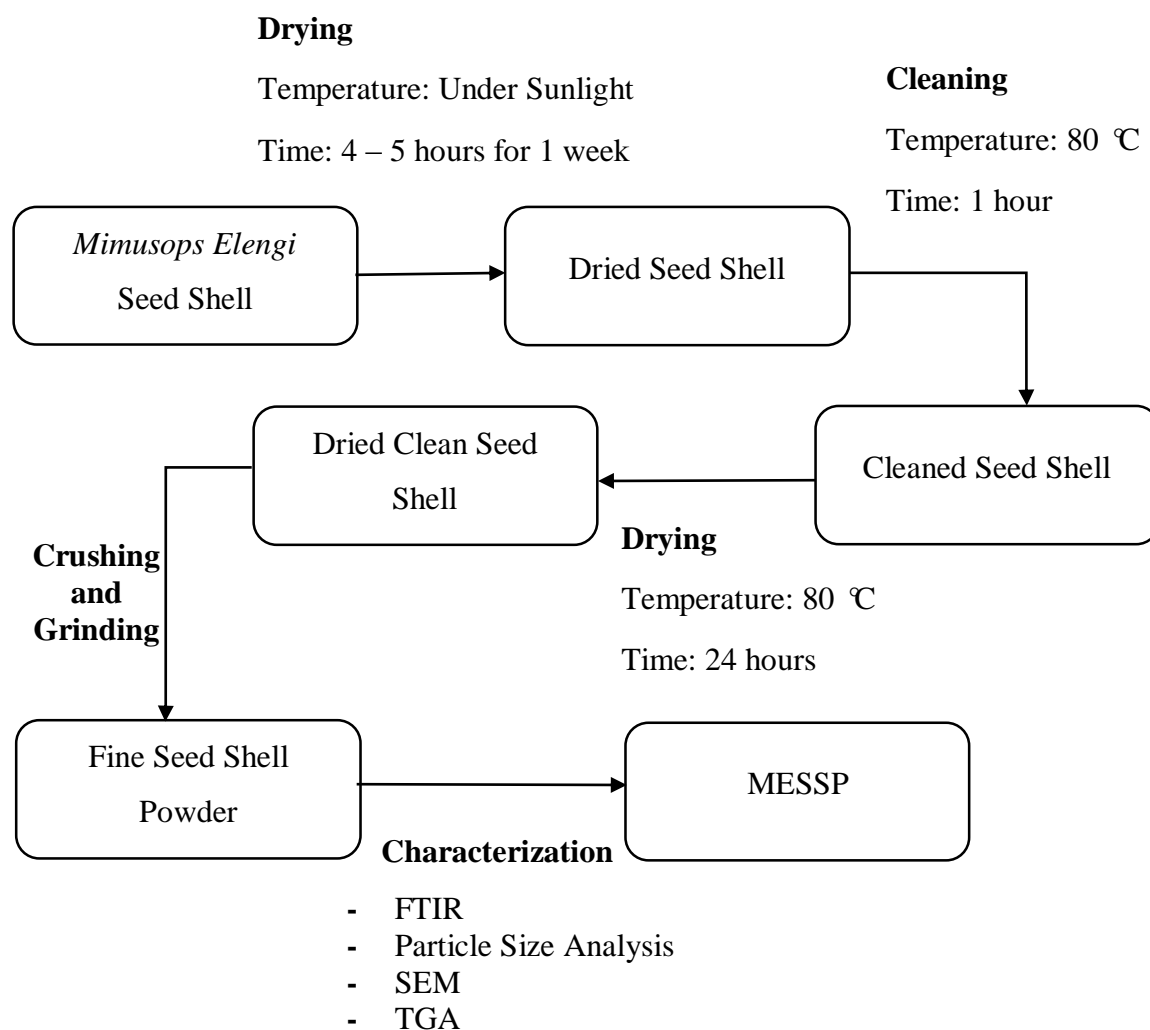


Figure 3.1: Flow Chart of MESSP Preparation

### 3.2.3 Miscellaneous Fillers

Other conventional or commercially used fillers such as carbon black (CB) N330, precipitated silica (Vulcasil C) and calcium carbonate (CaCO<sub>3</sub>) OMYACARB 2T-SA were all purchased from Bayer (M) Ltd and used as received.

### 3.3 Preparation of PP / MESSP Composites

PP resins and MESSP were pre-dried in vacuum oven for 24 hours at 80 °C. MESSP filled PP composites was produced by melt mixing method using a rheometer Brabender® Plastograph ® EC 815652 based on the compounding formulation as in Table 3.1. The mixing was carried out at melting temperature of PP (180 °C) for 10 minutes at 60 rpm. The graph of processing torque was obtained from the Brabender and was used to indicate the process-ability. PP / MESSP composites was then pressed into composite sheets using a hydraulic hot and cold press machine GT-7014-A30C at 180 °C. First the composites was preheated for 12 minutes and followed by compression for 4 minutes and finally cooling for 2 minutes. The preparation and testing of PP / MESSP composites is illustrated in Figure 3.2.

**Table 3.1: Compounding Formulation of PP / MESSP Composites**

<b>Materials</b>	<b>Composition (wt %)</b>				
PP	100	99	97.5	95	90
MESSP	0	1	2.5	5	10

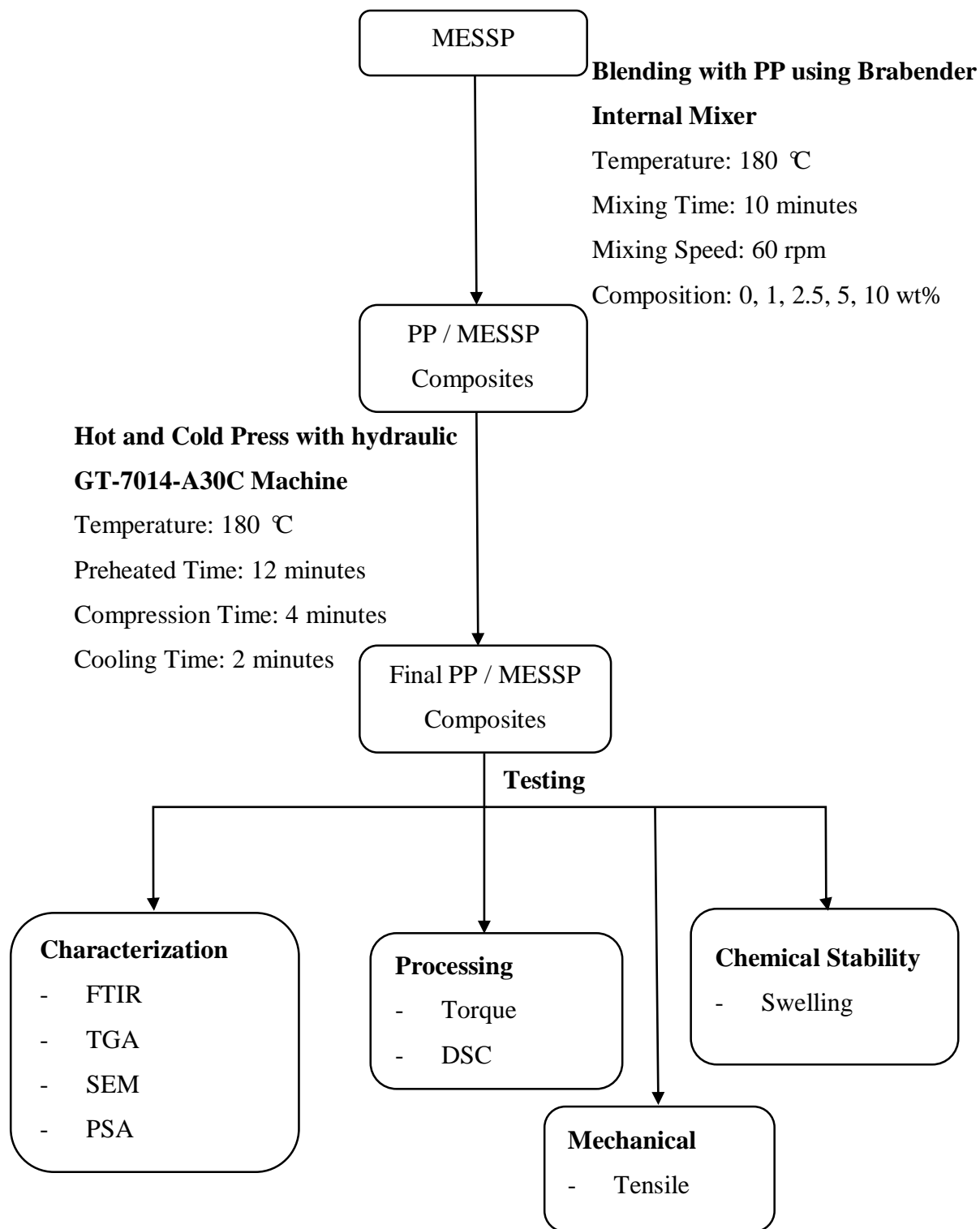


Figure 3.2: Flow Chart of Preparation and Testing of PP / MESSP Composites

### **3.4 Characterization of MESSP and PP / MESSP Composites**

#### **3.4.1 Particle Size Analysis (PSA)**

PSA was carried out by using Mastersizer 2000, Hydro2000 MU (A) to determine the particle size distribution of MESSP and other commercial fillers. Mean diameter and specific surface area of MESSP and other fillers were also obtained from the analysis.

#### **3.4.2 Fourier Transform Infrared Spectroscopy (FTIR)**

FTIR was carried out by using Perkin Elmer Spectrum ex1 to identify the types of chemical bonds and functional groups in MESSP and PP / MESSP composites. The analysis was carried out to determine the absorption band with a wavelength from 4000  $\text{cm}^{-1}$  to 400  $\text{cm}^{-1}$  with 4 scans at a resolution of 4  $\text{cm}^{-1}$ . MESSP will be mixed with KBr to prepare as MESSP pellet for the analysis.

#### **3.4.3 Scanning Electron Microscopy (SEM)**

The morphology of MESSP and PP / MESSP composites were observed by using SEM at accelerating voltage of 2 kV. Prior to scanning, the samples were placed on a disc and held in place using a double – sided carbon tape then coated with platinum particles to avoid sample charging. The model of equipment used will be JOEL JSM 6701F.

### 3.4.4 Thermogravimetric Analysis (TGA)

TGA was performed to determine the decomposition temperature and thus, the thermal stability of MESSP and PP / MESSP composites. Measurements were carried out under a nitrogen atmosphere using a heating rate of 20 °C / min from 30 to 600 °C using Metler Toledo TGA SDTA851 E.

## 3.5 Testing of PP / MESSP Composites

### 3.5.1 Differential Scanning Calorimetry (DSC)

Mettler Toledo TOPEM was used to determine the melting points, crystallinity and crystallizing temperatures of PP and PP / MESSP composites. The samples were heated from 25 °C to 300 °C at a rate of 10 °C / min under nitrogen flow of 10 mL / min and immediately cooling back to 25 °C. The degree of crystallinity is calculated using equation 3.1:

$$X_c^m = \frac{\Delta H_m}{W_p \times \Delta H_{100}} \times 100\% \quad (3.1)$$

where

$X_c^m$  = degree of crystallinity (%)

$\Delta H_m$  = Melting heat (J / g)

$\Delta H_{100}$  = Melting heat for 100% crystalline polypropylene, 207 J / g

$W_p$  = Weight fraction of polymer in sample

### 3.5.2 Swelling Resistance

PP / MESSP composites samples were cut into dumbbell shaped from the compression molded sheet and the swelling test was carried out using distilled water and toluene as a solvent in accordance with ASTM D471-79. The test pieces were weighed using an electronic balance and initial mass ( $M_i$ ) of the samples was recorded in grams. The test pieces were then immerse in distilled water and toluene for 72 hours and condition at 25 °C in dark place. After 72 hours, the test pieces were weighed again and the mass of the samples after immersion ( $M_s$ ) in distilled water and toluene was recorded. Water and solvent resistance of PP / MESSP composites were determined from the swelling percentage of samples in distilled water and toluene. The higher swelling percentage indicates the lower water and solvent resistance of PP / MESSP composites. Swelling percentage was calculated based on equation 3.2.

$$\text{Swelling Percentage} = [(M_s - M_i) / M_i] \times 100 \quad (3.2)$$

### 3.5.3 Tensile Test

According to ASTM D638, tensile test was carried out under ambient condition to measure the elastic modulus, ultimate tensile strength and elongation at break of PP / MESSP composites. The test was conducted by using Tinius Olsen H10KS-0748 with a 500 N load cell at a crosshead speed of 50 mm / min.

## **CHAPTER 4**

### **RESULTS AND DISCUSSION**

#### **4.1 Introduction**

This chapter consists of the results and discussion on characterization and analysis of MESSP and PP / MESSP composites in comparison to neat PP. Furthermore, all the results such as particle size analysis (PSA) of MESSP, processing torque, differential scanning calorimetry (DSC), fourier transform infrared (FTIR), water uptake and toluene swelling resistance test, thermogravimetric analysis (TGA), tensile test and scanning electron microscopy (SEM) of MESSP and PP / MESSP composites were interpreted with regards to the past research works done.

#### **4.2 Characterization of MESSP**

##### **4.2.1 Particle Size Analysis (PSA)**

Particle size analysis (PSA) is performed to understand the effect of particle size and distribution of particulate fillers which are very essential in enhancing the processing, thermal and mechanical properties of polymer composites (Lu and Xu, 1997). Figure 4.1 demonstrates the particle size distribution of MESSP as obtained from particle size

analysis. Based on the data obtained, the particle size of MESSP ranges from 0.0375 – 37.2425  $\mu\text{m}$  by sieving. The first distribution of particle size ranges from 0.0375 to 0.316  $\mu\text{m}$  while the second distribution ranges from 0.363 to 37.2425  $\mu\text{m}$ . The crushed MESSP was sieved using a 45  $\mu\text{m}$  sieve prior to compounding and this is to ease the process ability of PP / MESSP composites and prevent the tendency of agglomeration of large MESSP particles at higher loading.

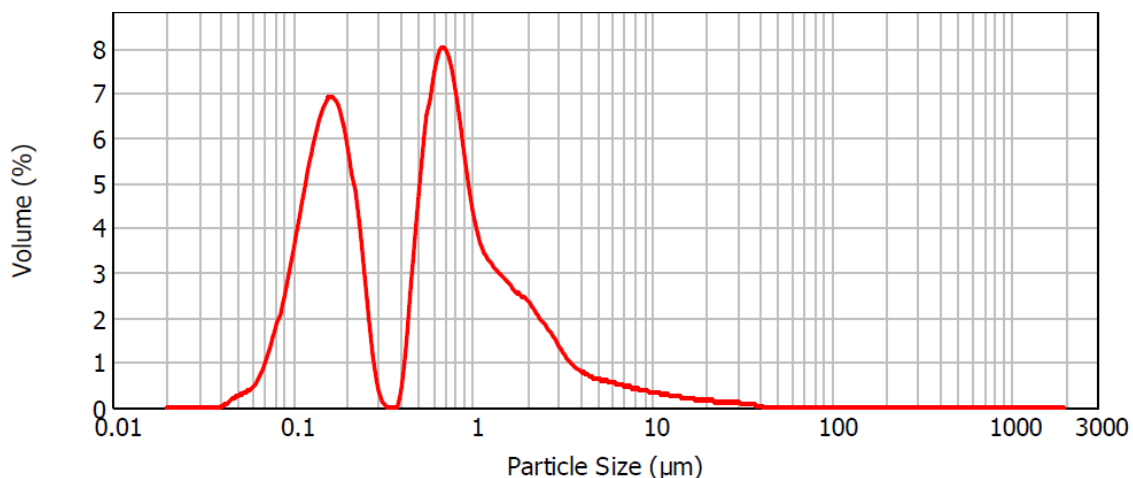


Figure 4.1: Particle Size Distribution of MESSP

In addition, Table 4.1 shows the other physical properties of MESSP as obtained through particle size analysis which is the mean diameter and specific surface area. By comparing the particle size distribution, MESSP has relatively narrow particle size distribution as compared to commercial fillers such as carbon black, silica and calcium carbonate. Narrow particle size distribution may lead to a more uniform pore structure than that of broader distribution (Bjørk et al., 2012). In addition, MESSP has the smallest mean diameter of 0.583  $\mu\text{m}$  while carbon black, silica and calcium carbonate have the mean diameter of 4.60  $\mu\text{m}$ , 20.02  $\mu\text{m}$  and 8.54  $\mu\text{m}$  respectively. This indicated that MESSP can be well dispersed and has low tendency to agglomerate between PP particles.

MESSP also has the highest value of specific surface area of 21.9  $\text{m}^2/\text{g}$  whereas carbon black, silica and calcium carbonate have specific surface area of 1.340  $\text{m}^2/\text{g}$ , 1.138



$\text{m}^2/\text{g}$  and  $0.896 \text{ m}^2/\text{g}$  respectively. Specific surface area is the total surface area exposed of a finely divided filler interacts with polymer matrix (Ash and Ash, 2007). Specific surface area works closely with shape, density, aspect ratio and particle size distribution of a particulate filler. Since MESSP possesses the highest value of specific surface area, it indicates that it has higher porosity or surface voids and more contact surface area available. This analysis suggest that MESSP has high potential to reinforce PP composites given that MESSP is compatible with PP matrix.

**Table 4.1: Physical Properties of MESSP, Carbon Black, Silica and Calcium Carbonate**

Particulate Fillers	Physical Properties		
	Particle Size Distribution ( $\mu\text{m}$ )	Mean Diameter ( $\mu\text{m}$ )	Specific Surface Area ( $\text{m}^2/\text{g}$ )
MESSP	0.0375 – 37.2425	0.583	21.9
Carbon Black	0.24 – 58.66	4.60	1.340
Silica	7.96 – 63.94	20.02	1.138
Calcium Carbonate	1.22 – 37.84	8.54	0.896

#### 4.2.2 Fourier Transform Infrared Spectroscopy (FTIR)

Fourier Transform Infrared Spectroscopy (FTIR) introduces quantitative and qualitative analysis for organic and inorganic samples. By generating an infrared absorption spectrum, FTIR able to diagnose the chemical bonds in a sample and develops an unique molecular fingerprint that can be used to screen and scan for many components (Intertek, 2016). Different samples will have its distinctive combination of molecules, and hence there is no compound that could produce similar infrared spectra.

The functional groups in MESSP was analyzed by FTIR. Table 4.2 tabulates the major infrared peaks of chemical structures on *Mimusops elengi* fruit based on Joseph and

George (2016). Whereas Figure 4.2 illustrates the FTIR spectrum of MESSP. O-H stretching which indicates MESSP is strongly bonded by intermolecular hydrogen bond was appeared as medium peak at the frequency of  $3335\text{ cm}^{-1}$ . The stretching vibrations of C-H group was found corresponding to the peak at  $2918\text{ cm}^{-1}$ . Besides, the peak at  $2100\text{ cm}^{-1}$  corresponded to  $\text{C} \equiv \text{C}$  stretching vibrations. The strong and well defined peak at  $1726\text{ cm}^{-1}$  appears due to aliphatic aldehyde  $\text{C}=\text{O}$  stretching. These explanation were also agreed by Bakar et al. and Matějka et al. when kenaf and jute fibers also shows similar infrared peaks at  $3650 - 3200\text{ cm}^{-1}$ ,  $2900 - 2700\text{ cm}^{-1}$  and  $1740 - 1720\text{ cm}^{-1}$ .

Furthermore, the presence of  $\text{C}=\text{C}$  symmetrical stretching was observed at the frequency of  $1611\text{ cm}^{-1}$  and  $1510\text{ cm}^{-1}$  respectively. The weak peak at  $1439\text{ cm}^{-1}$  was attributed to C-H bending or O-H bending (deformation). Apart from that, the absorption band identified at  $1362\text{ cm}^{-1}$ ,  $1235\text{ cm}^{-1}$  and  $1032\text{ cm}^{-1}$  indicated the presence of aromatic C-H group, C-H in plane bending and aliphatic C-O stretching, respectively. In the research of Jeyasundari et al., similar infrared spectrum also shown at  $1385.77\text{ cm}^{-1}$  as aromatic C-H group using *Mimusops elengi* flower extract.

**Table 4.2: FTIR Spectroscopy of MESSP (Stuart, 2004)**

Frequency Range ( $\text{cm}^{-1}$ )	Spectroscopic Assignments
3650 – 3200	O-H stretching
2900 - 2700	C-H stretching
2300 – 2050	$\text{C} \equiv \text{C}$ stretching vibration
1740 - 1720	Aliphatic aldehyde $\text{C}=\text{O}$ stretching
1650 – 1430	$\text{C}=\text{C}$ symmetrical stretching
1430	C-O-H in plane bending
1360 – 1250	Aromatic C-H group
1245	C-C stretching
1300 – 1000	Aliphatic C-O stretching

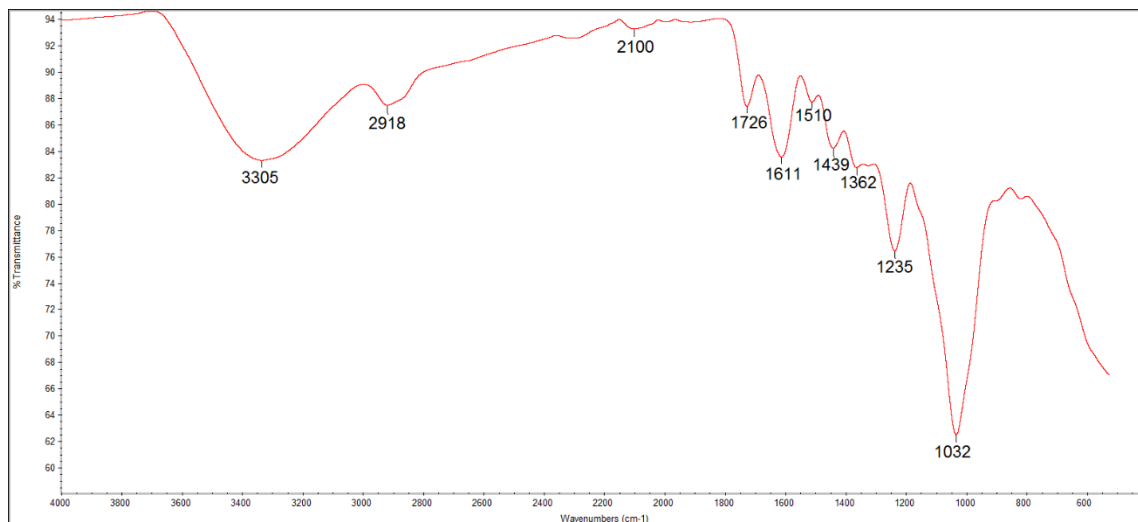


Figure 4.2: FTIR Spectra of MESSP

### 4.2.3 Thermogravimetric Analysis (TGA)

The thermal degradability of MESSP was identified by using TGA. From the data obtained, MESSP possessed low thermal stability as it almost fully decompose upon heating up from 30 – 600 °C. Thus, MESSP exhibited low thermal degradation temperature or low thermal stabilizing effect. Besides, there were 2 stages of thermal decomposition behavior where 2 temperature peaks were found in Figure 4.3. The first temperature peak was 65.73 °C and about 7.62 % of weight loss happened in this stage. This might be due to the volatilization of water or moisture in MESSP (Guan, Latif and Yap, 2013). Thermal decomposition of organic components such as cellulose, hemicellulose and lignin contained in MESSP might be contributed in the weight loss from 342 °C to 550 °C whereby the second peak was 342.08 °C and 75.83 % of weight loss was recorded. Almost zero weight loss was observed when MESSP was heating above 550 °C as shown in Figure 4.3. Similar findings can be obtained by Guan et al (2013) using raw sugarcane bagasse and corn husk to prepare activated carbon.

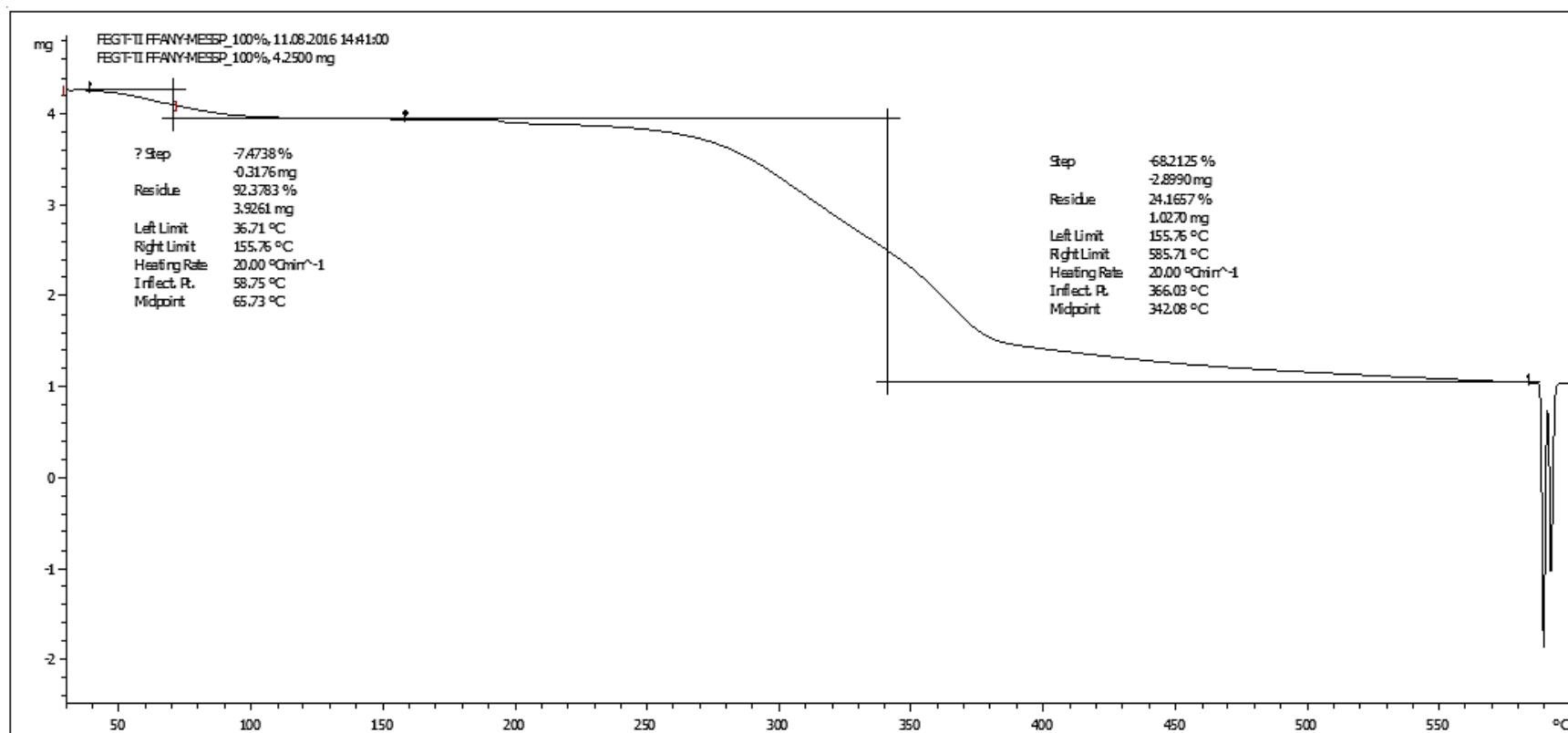


Figure 4.3: TGA Analysis of MESSP

#### 4.2.4 Scanning Electron Microscopy (SEM)

The morphology structures of MESSP were analyzed by using Scanning Electron Microscopy (SEM). SEM micrograph of MESSP surface at magnification 300x and 1000x were displayed in Figure 4.4 and Figure 4.5 respectively. As illustrated in Figures 4.4 and 4.5, MESSP exhibits less interaction between particles and tends to appear as an individual particles with irregular shape. MESSP has a relatively smooth surface with some agglomerated particles. In addition, MESSP does not showed any surface porosity on its structure but it showed small cracks on its surface which can be the responsible factor for its high specific surface area. The cracks on MESSP surface can be clearly observed in Figure 4.5, resulting in high specific surface area and physical interaction between PP and MESSP is possible through the matrix interlocking at the surface of MESSP.

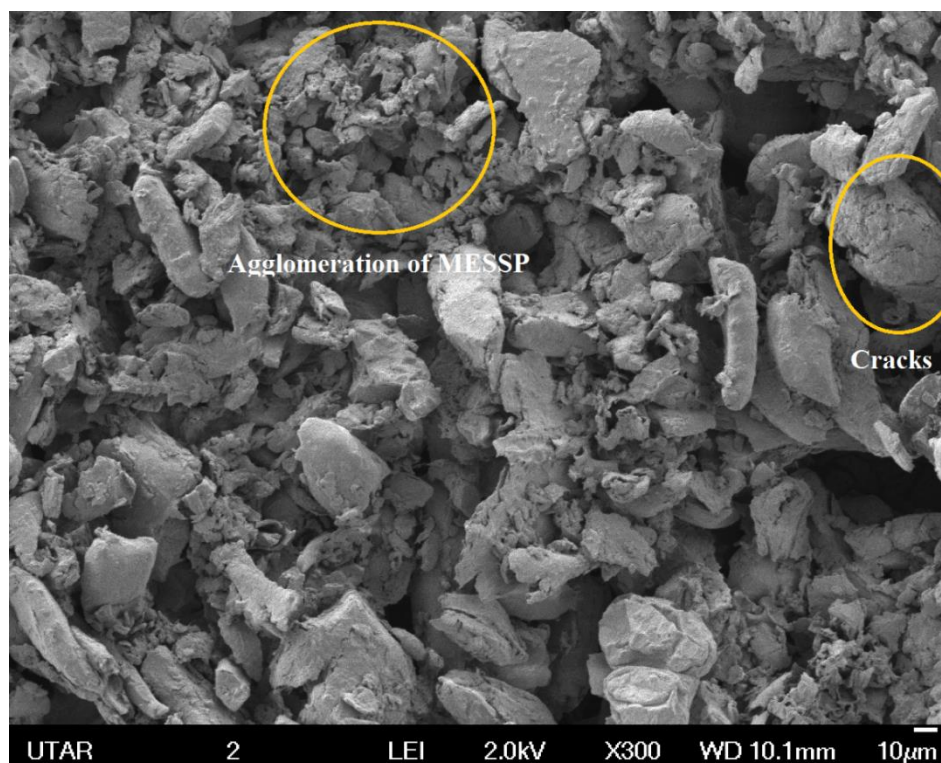


Figure 4.4: SEM Micrograph of MESSP at 300x Magnification

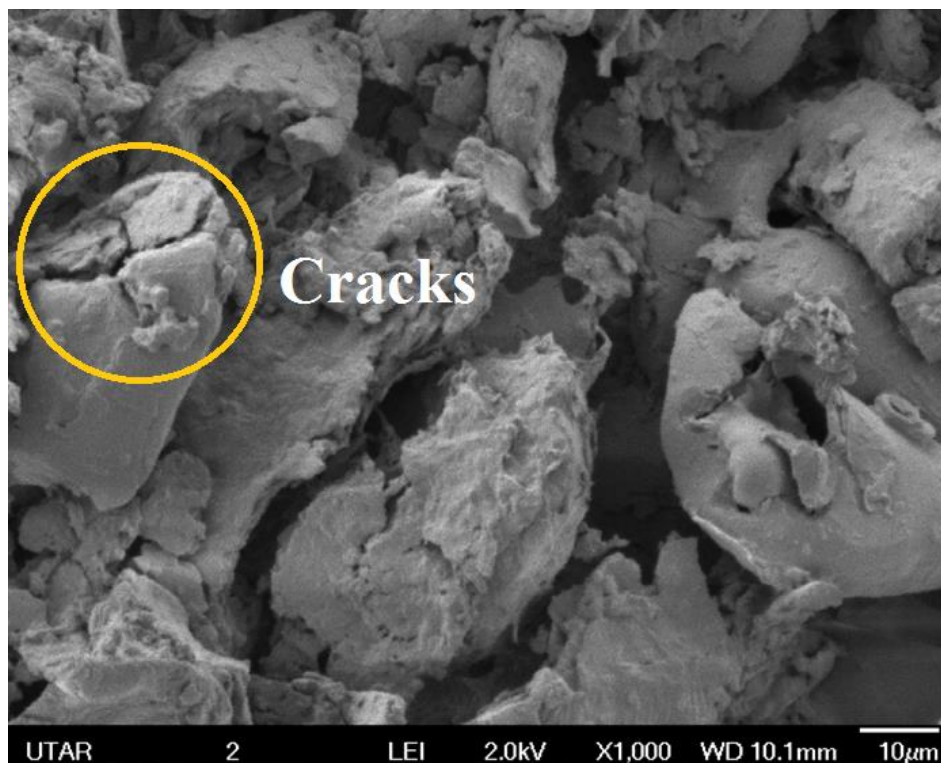


Figure 4.5: SEM Micrograph of MESSP at 1000x Magnification

### 4.3 Characterization and Testing of PP / MESSP Composites

#### 4.3.1 Fourier Transform Infrared Spectroscopy (FTIR)

The functional groups in PP / MESSP composite at different MESSP loading were analyzed by FTIR. FTIR analysis can be used to detect the possible chemical reaction that might occur between PP and MESSP. Table 4.3 tabulates the chemical structures of unfilled PP based on Mark (2006) and Stuart (2004). FTIR spectra of unfilled PP and PP loaded with different loadings of MESSP are shown in Figure 4.6. As demonstrated in Figure 4.6, peaks at all different composition of PP / MESSP composites possessed similar trend in FTIR spectra. PP possesses high peaks intensity at  $2915\text{ cm}^{-1}$  which indicates the presence of aliphatic C-H stretching. Similar peaks also observed in PP composites containing 1 to 10 wt% of MESSP. Besides,  $\text{CH}_2$  scissors vibration, symmetrical  $\text{CH}_3$

bending and CH<sub>2</sub> wagging also appeared at frequency of 1453 cm<sup>-1</sup> and 1372 cm<sup>-1</sup> respectively in unfilled PP and all PP / MESSP composites. Most of the peaks shown in the IR spectra of unfilled and filled PP show the presence of C-H bending of alkane groups (Mark, 2006).

**Table 4.3: FTIR Analysis of Unfilled PP (Mark, 2006)**

Frequency Range (cm <sup>-1</sup> )	Spectroscopic Assignments
3000 – 2800	Aliphatic C-H stretching
1634	C=C symmetrical stretching
1454	CH <sub>2</sub> scissors vibration
1372	Symmetrical CH <sub>3</sub> bending, CH <sub>2</sub> wagging vibration
1161	C-C stretching, CH <sub>3</sub> rocking vibration C-H bending
979	CH <sub>3</sub> rocking vibration, C-C stretching
898	CH <sub>2</sub> and CH <sub>3</sub> rocking vibration, C-H bending
838	CH <sub>2</sub> rocking vibration, C-CH <sub>3</sub> stretching
722	CH <sub>2</sub> rocking vibration

Table 4.4 tabulates the IR peaks of PP / MESSP composites at different frequencies. The peaks showed at different frequency ease the identification of functional groups in PP / MESSP composites. For instance, the absorption band in between 3650 – 3200 cm<sup>-1</sup> was clearly detected due to the stretching of O-H bond. This statement also agreed by Shao et al.'s research using three types of natural fiber reinforced composites. With the presence of peak at 1634 cm<sup>-1</sup>, it was identified O-H bending of absorbed water was appeared in the PP / MESSP composites (Fan, Dai and Huang, 2012). Furthermore, the appearance of aliphatic C-O stretching can also be determined from 1300 – 1000 cm<sup>-1</sup> (Stuart, 2004).

From the FTIR analysis, no new peaks have been detected in between PP and MESSP which confirms that there were no chemical reaction took place between PP and MESSP. Hence, it can be said that any possible improvement in the mechanical, thermal

or chemical properties of the composites can be credited to the physical interaction such as interlocking of PP chains at MESSP surface cracks. Besides, the increasing water swelling percentage of PP / MESSP composites is in good agreement with the presence of OH from moisture absorbed by PP / MESSP.

**Table 4.4: FTIR Analysis of PP / MESSP Composites (Mark, 2006; Stuart, 2004)**

<b>Frequency Range (cm<sup>-1</sup>)</b>	<b>Spectroscopic Assignments</b>
3650 – 3200	O-H stretching
3000 – 2800	Aliphatic C-H stretching
2900 – 2700	Aldehyde C-H stretching
1634	O-H bending of absorbed water
1454	CH <sub>2</sub> scissors vibration
1372	Symmetrical CH <sub>3</sub> bending, CH <sub>2</sub> wagging vibration
1161	C-C stretching, CH <sub>3</sub> rocking vibration C-H bending
1300 – 1000	Aliphatic C-O stretching
979	CH <sub>3</sub> rocking vibration, C-C stretching
898	CH <sub>2</sub> and CH <sub>3</sub> rocking vibration, C-H bending
838	CH <sub>2</sub> rocking vibration, C-CH <sub>3</sub> stretching
722	CH <sub>2</sub> rocking vibration



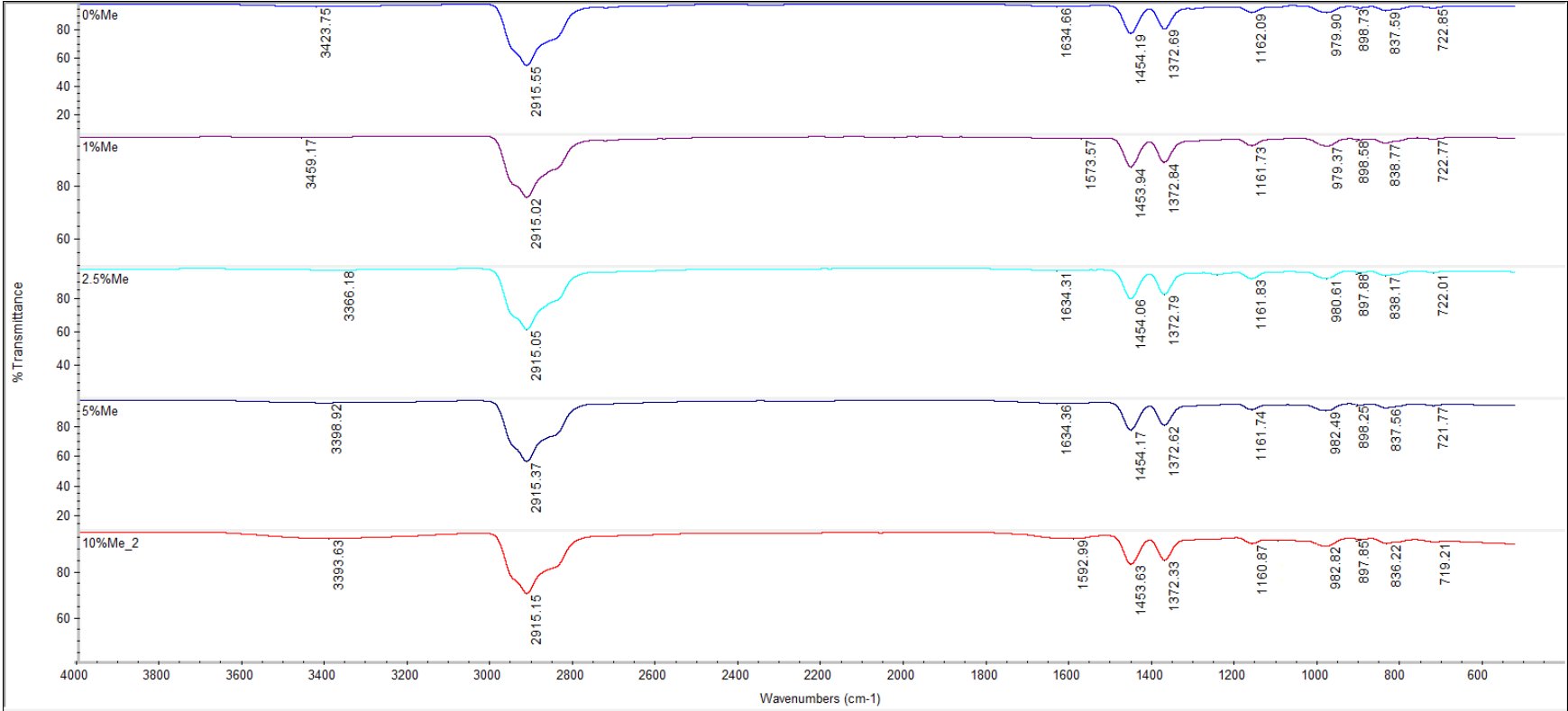


Figure 4.6: FTIR Spectra of PP / MESSP Composites at Different MESSP Loading

### 4.3.2 Processing Properties

The melt processing characteristic of PP / MESSP composites were reviewed through the melt mixing of PP pellets and MESSP powder in a Brabender Internal Mixer. In the processing of polymers, processing torque reveals the rheological properties of composites such as viscosity, process-ability and stiffness of the composites formed. It is necessary to understand and evaluate the rheological behavior of polymer composites as it resolves the melt process-ability of polymers and physical properties of the processed end-products (Aho, 2011). Nevertheless, the rheological properties greatly depending on the operating conditions such as temperature, pressure, flow and structural specification such as molecular weight, particle size and distribution (Silva et al., 2014).

During the mixing process, PP pellets melts upon heat absorption supplied by the high temperature plates surrounding it and mixed with MESSP. The shearing action between PP pellets tend to produce high frictional force, resulting in high shear stress and processing torque value. Hence, the loading torque which is the initial torque produced upon polymer discharge is highly depending on the amount of PP pellets. Based on Figure 4.7, the loading torque values reduces for 1 wt% MESSP loaded PP as compared to unfilled PP and it gradually increases back from 2.5 to 10 wt% loading. It was also discovered that the PP / MESSP composites have lower torque value as compared to unfilled PP excluding the 10 wt% of MESSP loading which has slightly higher loading peak of torque than that of unfilled PP. The low torque values of PP / MESSP compounds as compared to unfilled PP reveals the enhanced processing of PP in the presence of MESSP.

The reduction of loading torque of 1 wt% MESSP loaded PP as compared to unfilled PP is caused by the reason of decreasing the amount of PP fed into the hopper, resulting in the decrease of melt viscosity in the mixing chamber. This reduction also results in low shearing action between the molten PP and MESSP particles and less frictional force created during the mixing. Besides, the processing torque values of PP / MESSP composites is also affected by the particle size of MESSP. Due to the small

particle size of MESSP, negligible shearing action and frictional force was created, producing lower processing torque value at very low MESSP loading. Conversely, the frictional force between PP and MESSP increases when the loading of MESSP increases. More energy is required to melt PP and mix with high loading of MESSP, resulting in high processing torque. As a result, the loading torque value was increased from 1 to 10 wt% MESSP loading.

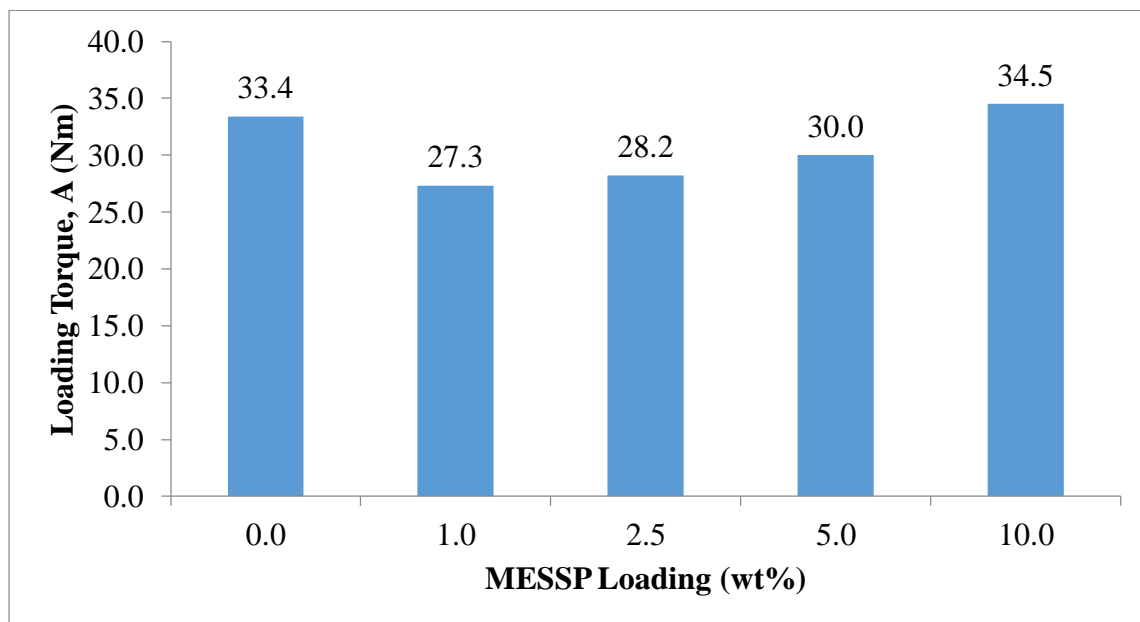


Figure 4.7: Loading Torque of PP / MESSP Composites at Various MESSP Loading

Figure 4.8 illustrates the stabilization torque of MESSP filled PP composite at different MESSP loading. Stabilization torque indicates the final torque produced upon formation of homogeneous mixture. The lower stabilization torque indicates easy processing and low stiffness of the compound as well as good dispersion of filler in the polymer matrix. The improvement of interaction between PP and MESSP particles can be proved by the growth in stabilization torque. The stabilization torque of PP / MESSP composites was detected to increase gradually with the increased MESSP loading. This can be explained by higher interfacial friction created between PP matrix and increasing MESSP loading, causing the polymer chain resist to move and increases the viscosity and stabilization torque (Viet et al., 2012). As compared to unfilled PP, the stabilization torque

of PP / MESSP composite is comparably or higher and it gradually increased with increasing MESSP loading. The increase can be due to the entrapment of PP chains at the surface of MESSP particles which restricts the chain movement subsequently results in higher stabilization torque. Thus, the optimum and comparable processing of PP / MESSP and neat PP is when the MESSP loading is at below 5 wt%.

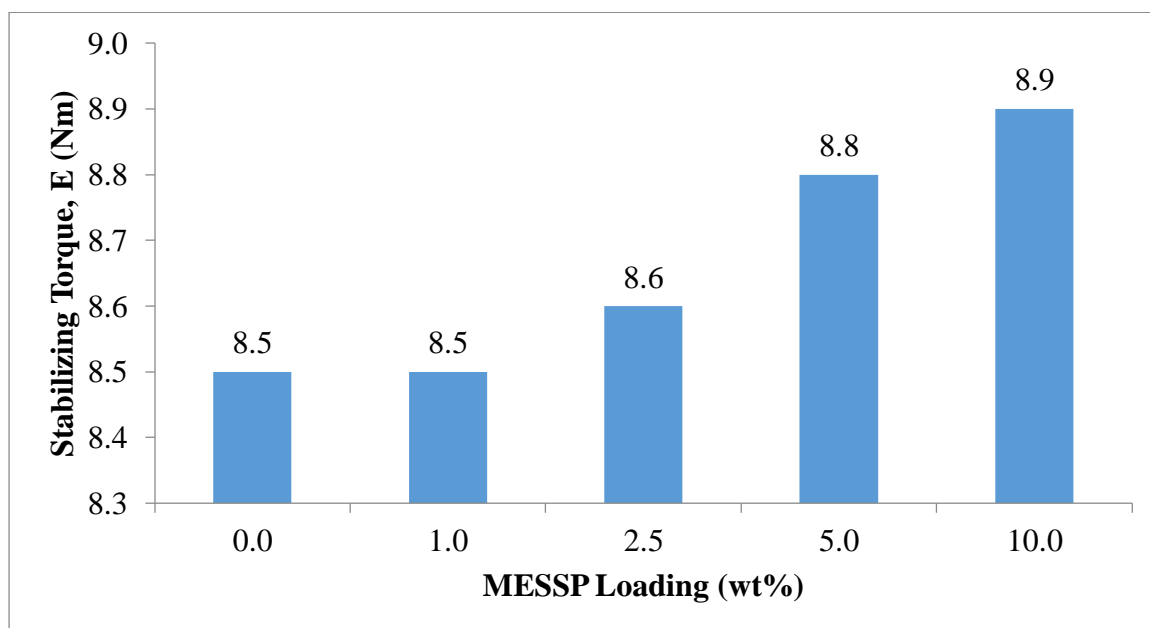


Figure 4.8: Stabilization Torque of PP / MESSP Composites at Various MESSP Loading

### 4.3.3 Differential Scanning Calorimetry (DSC)

Differential Scanning Calorimetry (DSC) is used to determine the melting point, crystallization behavior and degree of purity of a polymer sample. Table 4.5 illustrates the DSC results obtained for PP and PP / MESSP composites with increasing MESSP loading which were heated from 25 – 300 °C at heating rate of 10 °C / min and then cooled at the same rate. The effect of various MESSP loading on the melting temperature ( $T_m$ ), crystallization temperature ( $T_c$ ), melting enthalpy ( $\Delta H_m$ ) and degree of crystallinity ( $X_m^c$ ) of PP composites were measured.

As shown in Table 4.5, the melting temperature of composites substantially changed with increased MESSP loading. The melting temperature of unfilled PP at 170.92 °C is higher than the 1 wt% and 2.5 wt% MESSP filled PP composites which are 162.56 °C and 164.86 °C respectively. However, the melting temperature was slowly increased to 175.40 °C for 10 wt% of MESSP loading. The decreasing trend was also found on the enthalpy of melting of PP / MESSP composites from 101.43 J/g to 84.99 J/g suggested that MESSP in the PP composite absorbs more heat energy than the PP thermoplastic polymer resulting in higher  $T_m$  of PP / MESSP composites at higher loading (Tisserat et al., 2014).

From literature, the heat of crystallization of 100% crystalline PP is 207 J/g (Akinci, 2009). Bouza et al. (2007) suggested that the decrement in the crystallization temperature can be due to the reduction of nucleating activity by filler particles in the crystallization of polymers. As shown in Table 4.5, the crystallization temperature of 1 wt% MESSP filled PP decreases from 125.79 °C to 116.22 °C, resulted by the presence of MESSP which able to promote the surface nucleation sites and causes the crystallization of PP matrix to occur at lower temperature. However, the crystallization temperature of the composite was increased again to 127.05 °C at 10 wt% MESSP loading. This might be due to the higher amount of MESSP which tend to retard the formation of nucleus upon crystallization resulting in crystallization to occur at higher temperature.

Moreover, the small particle size of MESSP which can be easily dispersed in PP matrix has restricted the growth of crystalline structure and caused the overall reduction in degree of crystallinity of the composites from 49% for unfilled PP to 45.620% for 10 wt% MESSP filled PP. The presence of MESSP can be attributed to the resistance of the polymer matrix to flow and eventually increased the viscosity of the composites (Nurshamila et al., 2012). When the chain mobility of PP restricted to flow freely, the growth of crystalline structure will be restrained, causing in low crystallinity of PP / MESSP composites. The reduction in degree of crystallinity confirms that higher processing torque is required to ease the process ability of composites with increasing MESSP loading.

**Table 4.5: Data of DSC Analysis of Unfilled PP and PP / MESSP Composites**

MESSP Loading (wt%)	$W_p$	$T_m$ (°C)	$T_c$ (°C)	$\Delta H_m$ (J/g)	$X_m^c$ (%)
0	1.000	170.92	125.79	101.43	49.000
1.0	0.990	162.56	116.22	90.27	44.049
2.5	0.975	164.86	126.26	54.72	27.113
5.0	0.950	170.96	126.58	91.58	46.570
10.0	0.900	175.40	127.05	84.99	45.620

#### 4.3.4 Swelling Test in Water and Toluene

Swelling test in water was conducted to determine the water absorption capability of PP / MESSP composite as compared to PP. MESSP is an organic filler which has surface cracks and able to absorb water. The water absorption capability depends on MESSP properties such as particle size, surface area exposed, porosity and hydroxyl group within the chemical structure (Acevedo et al., 2016). Besides, swelling test in water can also help to conclude the stability of MESSP in PP matrix in the presence of moisture.

Figure 4.9 shows the water absorption of PP / MESSP composites at different MESSP loading. It can be clearly seen that the water absorption percentage of PP / MESSP composites increased gradually from 0 to 10 wt% MESSP loading. The water permeability degree of the composites increased with increasing filler loading is due to the formation of hydrogen bonding between free hydroxyl groups on MESSP cellulose molecules and water molecules (Demir et al., 2006). When MESSP comes in contact with moisture or water, hydrogen bonding will be formed between oxygenated groups of MESSP and water molecules. Hence, MESSP plays the role as the medium of water to be absorbed into the polymer composites. In contrast, PP is hydrophobic and non-polar in nature which has lower degree of water permeability. PP / MESSP composites with 10 wt% of MESSP loading has more contact surface area to form hydrogen bond with water molecules compared to pure PP and PP / MESSP composites with lower MESSP loading resulting

in absorption of more water and the highest water uptake capacity. However, addition of MESSP up to 10 wt% does not show a significant effect on water absorption by which there were only an increment of about 0.17% of water uptake as compared to neat PP.

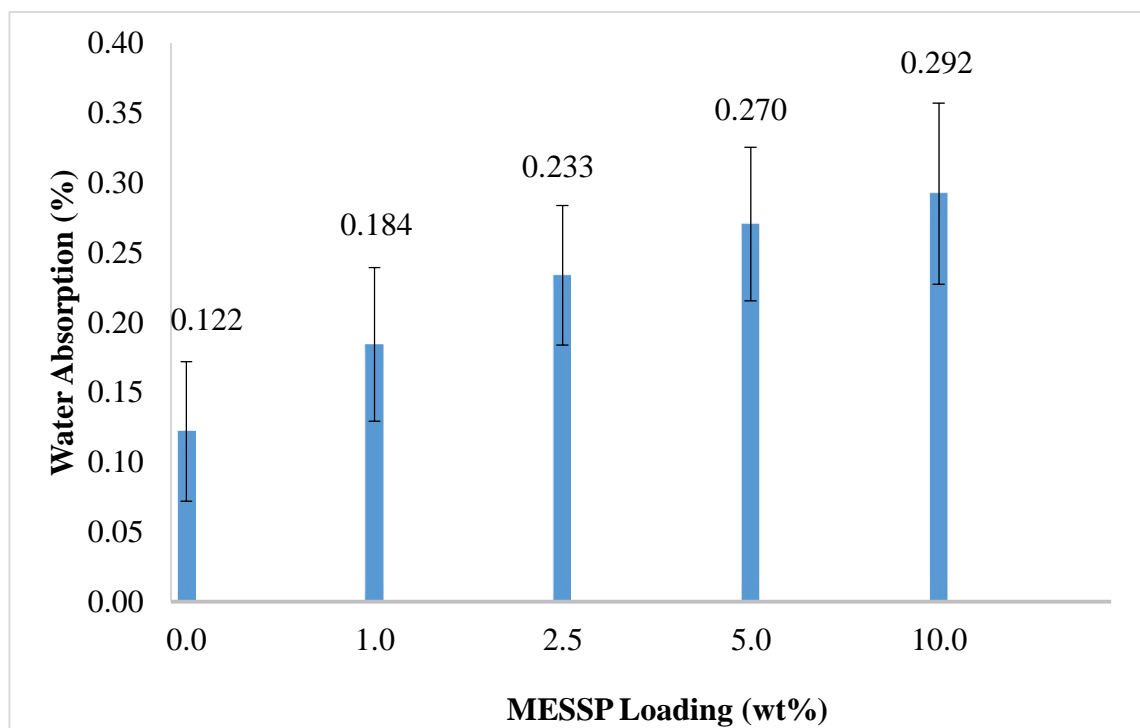


Figure 4.9: Water Absorption Percentage of PP / MESSP Composites at Different MESSP Loading

As mentioned before, PP is hydrophobic and has strong attraction towards non-polar organic solvent such as toluene. Therefore, swelling test in toluene was carried out to determine the toluene absorption capability of PP / MESSP composite as compared to PP. Figure 4.10 demonstrates the toluene absorption of PP / MESSP composites at different MESSP loading. It can be clearly observed that the toluene absorption percentage of PP / MESSP composites decreased gradually from 0 to 10 wt% MESSP loading. By comparison, unfilled PP has the highest degree of toluene permeability as compared to PP / MESSP composites. With increasing MESSP loading, the amount of PP was reduced and hence reduction in the toluene absorption percentage can be observed. The lowest absorption recorded at 10 wt% MESSP was 8.4%. Addition of MESSP also reduces the

path for the penetration of toluene into PP by blocking the absorption pathway. Thus, the overall amount of toluene absorbed into PP matrix is reduced in comparison to the unfilled PP which has more exposed path for toluene absorption.

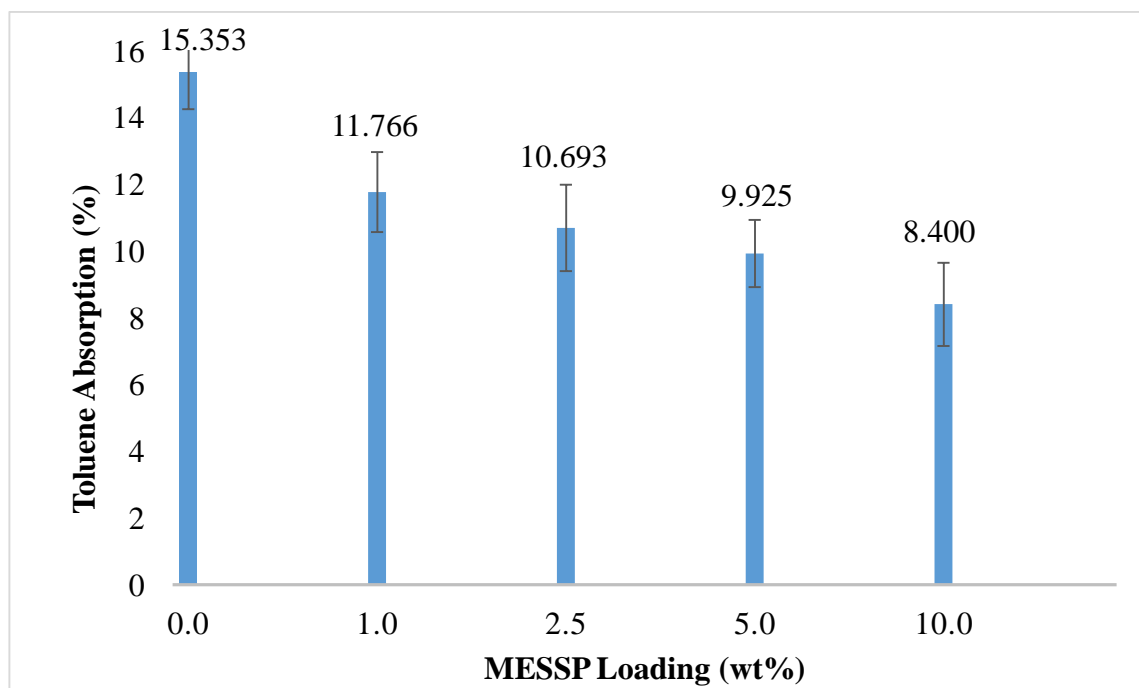


Figure 4.10: Toluene Absorption Percentage of PP / MESSP Composites at Different MESSP Loading

#### 4.3.5 Thermogravimetric Analysis (TGA)

Figure 4.11 shows the weight loss percentage of PP / MESSP composites at different MESSP loadings. Based on the statement by Zou et al. (2004), oxidation will start from the polymer before the filler starts to degrade and burn out in the composites. In this research, MESSP will start to degrade after PP is oxidized. Based on Figure 4.11, the composites start to degrade upon heating at 170 °C and undergoes the second thermal degradation about 372 °C where the lignocelulosic components in MESSP started to break off. Thus, PP / MESSP composites will undergo the first thermal decomposition which constituted by PP while the second degradation is constituted by MESSP itself.



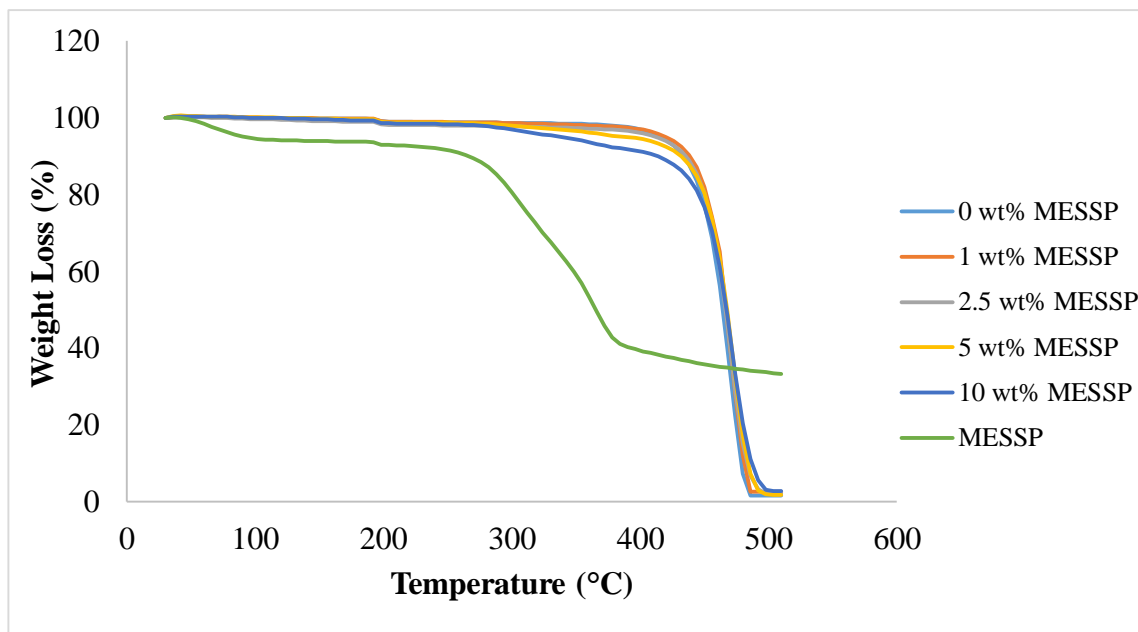


Figure 4.11: TGA Analysis of PP / MESSP Composites at Different MESSP Loading

The incorporation of MESSP into PP has increased the thermal stability of PP / MESSP composites. This can be proven by the analysis tabulated in Table 4.6 whereby 10 wt% MESSP filled PP has the highest solid remaining residue. The weight loss percentage of PP / MESSP composites decreases gradually with increasing MESSP loading. In comparison, the thermal stability enhancement increased gradually with increasing MESSP loading. 1.8 % of increment in the thermal stability enhancement can be observed when PP is mixed with 10 wt% of MESSP. Therefore, it can be said that the addition of MESSP in PP improved the thermal stability of PP / MESSP composites and it is aligned with the findings performed by Granda et al. (2016) using PP reinforced with *Leucaena collinsii* (LCN).

According to Ismail and Mathialagan (2011), the char residue produced will block the diffusion of the volatile decomposition products, resulting in the increase of thermal stability of polymer composites. Therefore, the higher the loading of MESSP, the higher the amount of residue formed, the more blocking of volatile by-products of combustion, the higher the thermal stability of PP / MESSP composites. Similar enhancement of

thermal stability also shown by the increase of temperature at maximum weight loss as shown in Table 4.6.

**Table 4.6: TGA Analysis of PP / MESSP Composites at Different MESSP Loading**

<b>MESSP Loading (wt%)</b>	<b>Temperature at 50% mass loss ( °C)</b>	<b>Maximum Weight Loss (%)</b>	<b>Residue (%)</b>	<b>Thermal Stability Enhancement (%)</b>
0	464.0	92.802	7.198	0
1.0	466.8	88.006	11.994	0.666
2.5	466.4	85.057	14.943	1.076
5.0	467.6	85.731	17.269	1.399
10.0	467.2	79.597	20.403	1.835
Raw MESSP	365.0	65.684	34.317	3.767

#### 4.3.6 Tensile Test

Table 4.7 summarizes the results obtained through tensile testing which is the ultimate tensile strength, tensile modulus and elongation at break of PP / MESSP composites at different MESSP loading. Ultimate tensile strength is also known as tensile strength, interprets as the maximum stress of a sample able to withstand before failure happened after applied force was released (Herz, 2012). It strongly depends on the particle size, particle loading and particle/matrix interfacial adhesion (Fu et al., 2008). It can be observed from Figure 4.12 that the ultimate tensile strength of PP / MESSP composites decreased gradually from 0 to 10 wt% MESSP loading at 30.07 MPa to 24.07 MPa.

In general, the mechanical properties of polymer composites can be affected by the elemental characteristic of fillers resulting in the adhesion between two different materials to be varied (Das et al., 2015). In this case, the incorporation of MESSP into PP matrix caused PP / MESSP composite to exhibit low tensile strength as compared to

unfilled PP. Due to the hydrophilic nature of MESSP incorporated into hydrophobic nature of PP matrix, incompatibility between the filler and matrix occurred and formed a weak interfacial interaction between PP and MESSP, resulting in minimum stress was transferred across the interphase of filler matrix (Nurshamila et al., 2012).

Besides, the weak interface of the composite may act as a stress concentration point instead of a reinforcement to the polymer matrix and caused MESSP to either agglomerate or function as non-reinforcing filler (Pang et al., 2015). High MESSP loading may result in poor dispersion of MESSP in the PP matrix and eventually caused low tensile strength. This results is in line with the SEM observation which reveals the agglomeration of MESSP at higher loading which will be discussed at the SEM observation part. Similar results also reported by Muniandy et al. (2012) by which tensile strength of natural rubber reduced with the addition of rattan powder and this is due to the poor adhesion between the filler and matrix.

**Table 4.7: Tensile Properties of PP / MESSP Composites at Different MESSP Loading**

<b>Parameter</b>	<b>MESSP Loading</b>				
	0	1.0	2.5	5.0	10.0
UTS (MPa)	30.07	27.54	26.88	24.58	24.07
E-Modulus (MPa)	983.00	1030.00	1050.00	1101.00	1127.00
Elongation at Break (%)	191.30	28.44	27.18	23.20	18.11

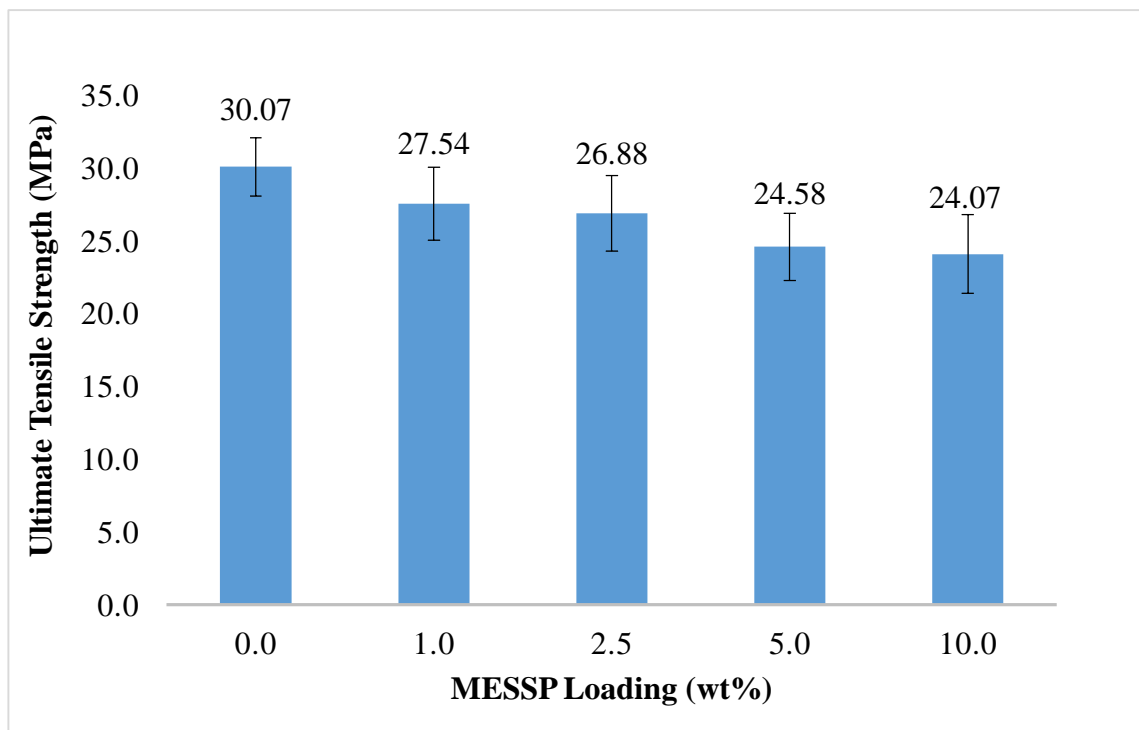


Figure 4.12: Ultimate Tensile Strength of PP / MESSP Composites at Different MESSP Loading

Figure 4.13 illustrates the E-modulus of PP / MESSP composites at different MESSP loading. E-modulus or tensile modulus refers to the stiffness of a composite and its resistance to fracture when stress is applied (Fu et al., 2008). According to Pang et al. (2015), the higher the tensile modulus values, the stiffer the composites are. Tensile modulus of a polymer composite highly relying on the stiffness of filler itself (John and Thomas, 2008). In this study, the stiffness of PP / MESSP composite was enhanced by the inclusion of MESSP in the PP matrix. This can be proven by Figure 4.13 which shows that the tensile modulus of the composites were increased gradually with increasing MESSP loading. PP / MESSP composites was hindered from moving freely due to the presence of MESSP in the matrix and hence improves the rigidity of the composite (Pang et al., 2015). A similar observation was noted by Bakar et al. (2015) where there is an increase in the tensile modulus of PVC / EVA matrix in the presence of kenaf fibers.

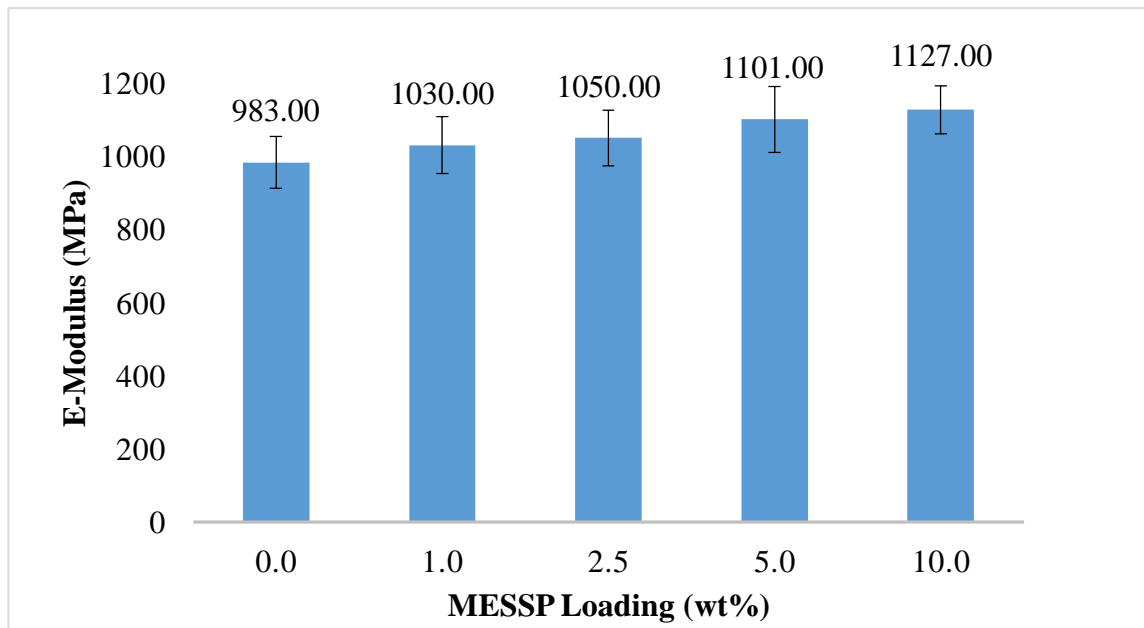


Figure 4.13: E-Modulus of PP / MESSP Composites at Different MESSP Loading

Figure 4.14 shows the elongation at break of PP / MESSP composites with increasing MESSP loading. Based on Fu et al. (2008), particulate fillers tend to increase the brittleness of polymer composite in ductile matrices if there is no or weak interfacial adhesion between the filler and polymer. Due to the increasing MESSP content in the composite, PP chain was inhibited to move freely and causes the deformability of the composites to diminish. PP / MESSP composites became harder to deform with inclining MESSP loading when stress is applied (Pang et al., 2015). As a consequence, elongation at break of PP / MESSP composites decreased from 0 to 10 wt% MESSP loading at 191.30% to 18.11% as the interfacial adhesion between MESSP and PP matrix was weak. Besides, high rigidity of composites due to high filler loading and agglomeration of fillers which tend to act as the rigid part in polymer may also cause the reduction in elongation at break.

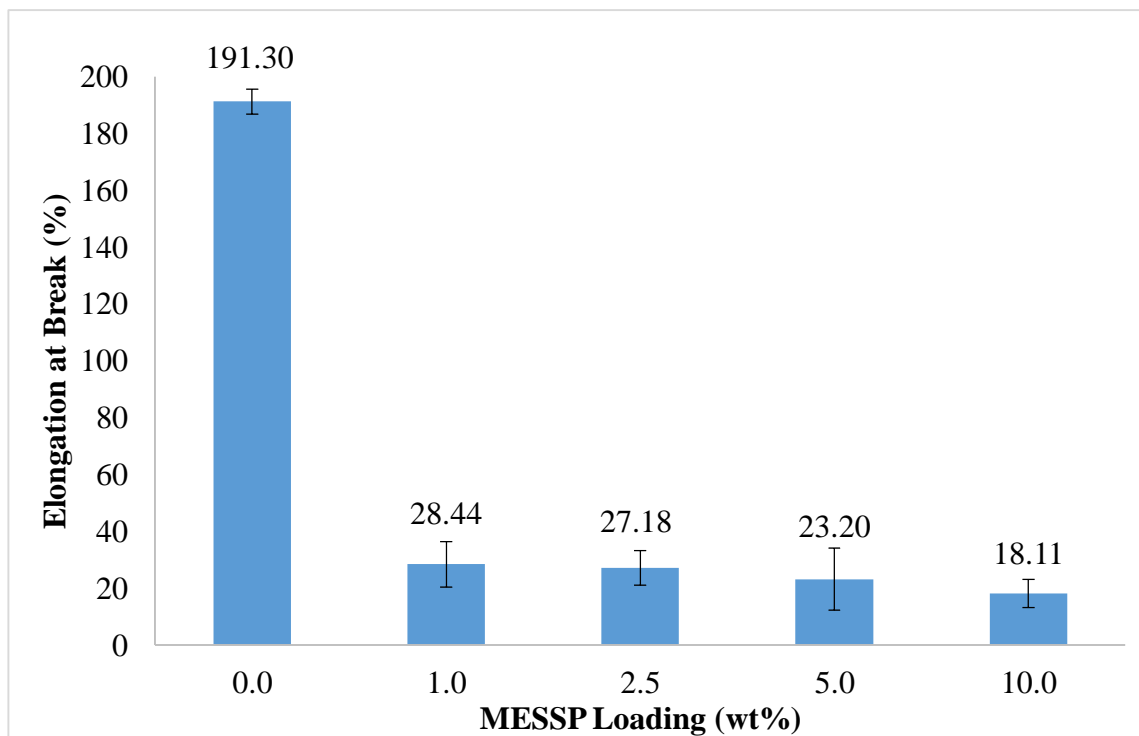


Figure 4.14: Elongation at Break of PP / MESSP Composites at Different MESSP Loading

#### 4.3.7 Scanning Electron Microscopy (SEM)

The morphology of PP / MESSP composites at 0 wt%, 2.5 wt% and 10 wt% MESSP loading were analyzed by SEM. Figure 4.15 (a) shows the morphology of unfilled PP, whereas Figure 4.15 (b) and Figure 4.15 (c) shows the morphology of PP / 2.5 wt% MESSP and PP / 10 wt% MESSP respectively. In contrast, unfilled PP has semi-rough and fibrous surface as compared to PP / 2.5 wt% MESSP and PP / 10 wt% MESSP. Based on this surface characteristic, it showed that PP particles were distributed well in its matrix and had strong interfacial adhesion to the particles. Thus, unfilled PP demonstrates less crack propagation and capable to withstand high elongation before fracture. This theory is in line with the tensile test's results obtained which showed that unfilled PP is flexible material with high tensile strength and elongation at break but low tensile modulus.

Similarly, PP / 10 wt% MESSP has relatively rougher surface but lesser matrix tearing than unfilled PP and PP / 2.5 wt% MESSP and can be clearly seen in Figure 4.15 (b) and Figure 4.15 (c). Due to the agglomeration of MESSP in the matrix, matrix tearing was produced and it indicated that there is poor adhesion between PP and MESSP and poor dispersion of MESSP in PP (Miguez Suarez, Coutinho and Sydenstricker, 2003).

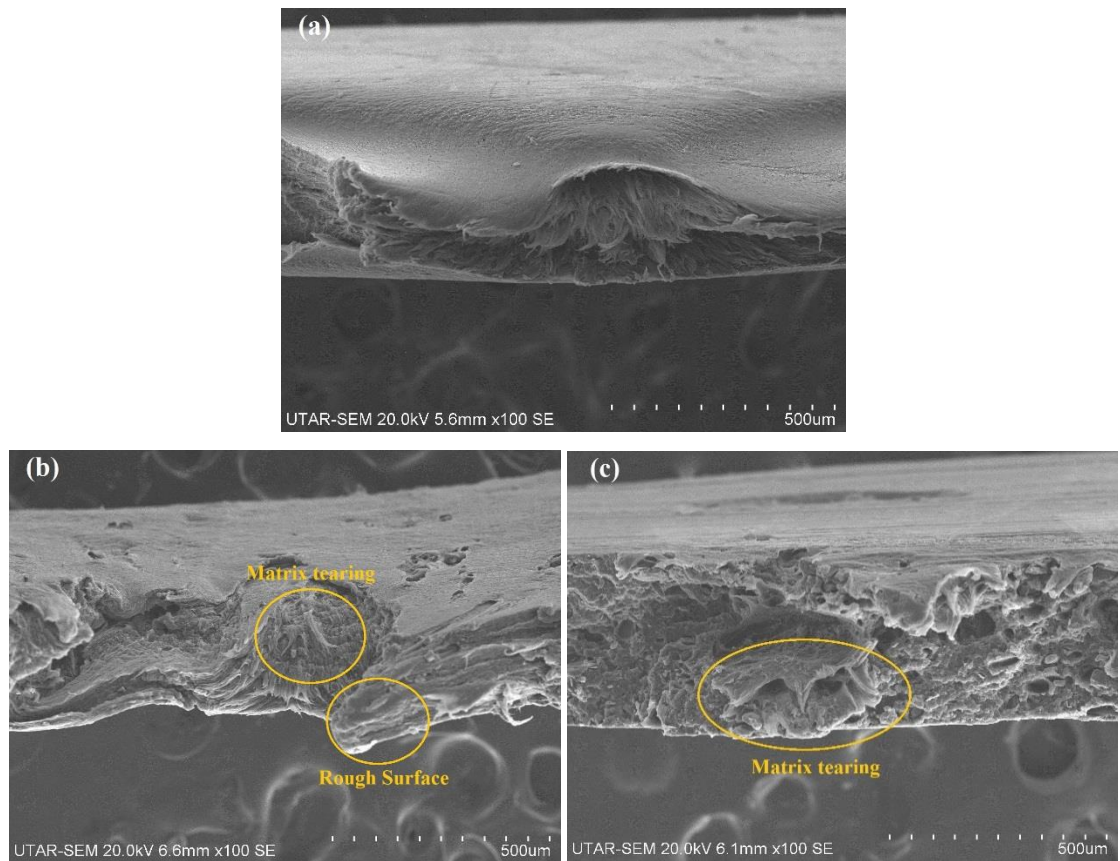


Figure 4.15: SEM Micrograph of Tensile Fracture of (a) Unfilled PP, (b) PP / 2.5 wt% MESSP and (c) PP / 10 wt% MESSP at 100x Magnification

In addition, Figure 4.16 (a) shows that the surface of PP / 2.5 wt% MESSP consists of a lot of micropores. This might have been due to the water moisture and air bubbles entrapped in the composite matrix and caused the presence of micropores in the morphology. Besides, PP / 10 wt% MESSP shows the presence of holes or voids after MESSP particles were pulled out of the composites upon loading cohesively, producing

weak interfacial interactions between PP and MESSP particles. The holes also act as the stress concentration points and initiates the potential of the composites to crack, causing a reduction in tensile strength up to 10 wt% MESSP as portrayed in the tensile test's results. Similar trend was observed by Ismail and Mathialagan (2011) in their studies on bentonite (Bt) filled EPDM composites which showed that Bt particles were pulled out of the composites upon loading, creating pores and voids and it illustrates weak interfacial adhesion as the Bt loading increased.

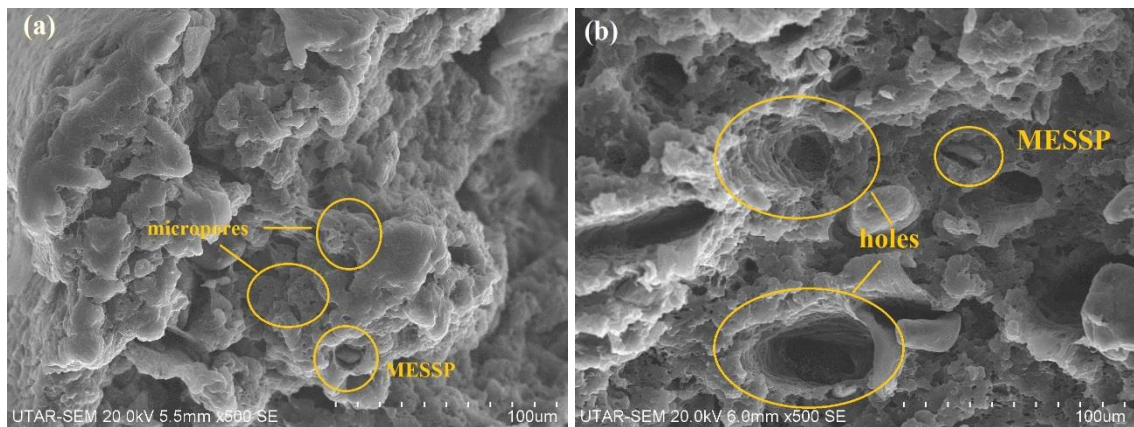


Figure 4.16: SEM Micrograph of Tensile Fracture of (a) PP / 2.5 wt% MESSP and (b) PP / 10 wt% MESSP at 500x Magnification

As demonstrated in Figure 4.17 (a) and (b), air gaps were showed in the morphology of PP / 2.5 wt% and 10 wt% MESSP loading. The presence of air gaps reveals that there is no chemical interaction between PP and MESSP particles in the composites and the air gaps also act as the cracking propagation path when stress is applied. According to Riley et al. 's statement, stiffness of a composite greatly relies on the filler loading, filler's aspect ratio and filler modulus. In order to obtain high stiffness material, it requires fillers with high aspect ratio at high loading. Hence, composite with 10 wt% of MESSP loading achieved the highest value of E-modulus in the tensile test due to highest MESSP loading and MESSP is more rigid than PP.



Furthermore, Kohls et al. found that the interaction between filler and polymer can be affected by the occlusion of polymer which is trapped between or within the filler voids. This can be seen in Figure 4.16 (a) and Figure 4.17 (b) where the infiltration of MESSP at the PP matrix surface and the interactions between PP and MESSP acts as part of the polymer network enhances the stiffness of the composites. This results or observation is in line with the gradual increase in tensile modulus and reduction in elongation at break as the amount of MESSP increase.

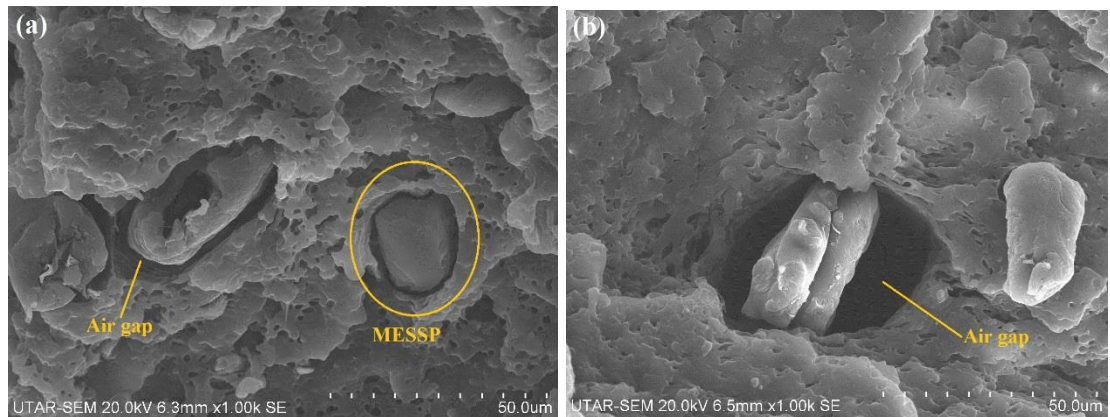


Figure 4.17: SEM Micrograph of Tensile Fracture of (a) PP / 1 wt% MESSP and (b) PP / 10 wt% MESSP at 1000x Magnification

## CHAPTER 5

### CONCLUSION AND RECOMMENDATIONS

#### 5.1 Conclusion

MESSP was successfully produced by drying, crushing and sieving of seed shell of *Mimusops elengi* fruit. The mean diameter of MESSP is 0.583  $\mu\text{m}$ , specific surface area is 21.9  $\text{m}^2/\text{g}$ , low thermal stability and SEM showed irregular shaped particles with many surface voids or cracks. Besides, MESSP filled PP composites at 0, 1, 2.5, 5 and 10 wt% of MESSP loading were successfully produced through melt blending using a Brabender internal mixer with 10 minutes of processing time at 180  $^{\circ}\text{C}$  and 60 rpm.

In this research, MESSP had showed more of non-reinforcing behavior when used as filler in PP by which tensile modulus, toluene resistance, thermal stability and processing were enhanced up to 10 wt% loading. However, the ultimate tensile strength, elongation at break and water absorption percentage were compromised. The enhancement in physico-mechanical properties of PP / MESSP is solely based on physical interaction and no chemical interaction due to the difference in surface functional group of PP and MESSP.

The optimum loading of MESSP to produce the best PP / MESSP composite is 2.5 – 5 wt% which shows comparable results of processing torque, TGA, DSC, toluene resistance and tensile modulus as compare to unfilled PP. Further addition of MESSP

above 5 wt% results in deterioration on tensile properties although thermal, chemical and process-ability were improved.

## **5.2 Recommendations**

In order to improve the outcome of this research, few recommendations are made such as:-

- Higher loading and larger particles size of MESSP should be used to produce PP / MESSP composites. This would greatly improve the interaction between MESSP and PP, producing high stiffness of PP / MESSP composites.
- Several modification and surface pre-treatment such as addition of UV stabilizers and fire retardants, surface treatment by through alkalization and others can be used to ease the process-ability of PP / MESSP composites. Coupling agent such as silane can be added during the processing to enhance the adhesion between MESSP filler and PP matrix.

## REFERENCES

- Acevedo, M., Tapia, A., Correa, J., Ricardo, R. and Realpe, A. (2016). Characterization of Recycled Polypropylene Composite Material Reinforced with Wood Flour using SEPS-gMAH as Coupling Agent. *International Journal of Engineering and Technology*, 8(2), pp.1397-1405.
- Adhesiveandglue.com, (2016). *Thermoplastic - Definition and examples of thermoplastic*. [online] Available at: <http://www.adhesiveandglue.com/thermoplastic.html> [Accessed 29 Feb. 2016].
- Aho, J. (2011). *Rheological Characterization of Polymer Melts in Shear and Extension: Measurement Reliability and Data for Practical Processing*. Tampere University of Technology.
- Akinci, A. (2009). Mechanical and structural properties of polypropylene composites filled with graphite flakes. *Archives of Material Science and Engineering*, 35(2), pp.91-94.
- APME, (2007). *Plastics a material of choice for the packaging*. 1st ed. [ebook] Association of Plastics Manufacturers in Europe, pp.1-10. Available at: <http://www.plasticseurope.de/cust/documentrequest.aspx?DocID=56793> [Accessed 1 Mar. 2016].
- Azwa, Z., Yousif, B., Manalo, A. and Karunasena, W. (2013). A review on the degradability of polymeric composites based on natural fibres. *Materials & Design*, 47, pp.424-442.
- BagsBeGone.com, (2012). *The Plastic Problem*. [online] Available at: <https://bagsbegone.com/resources/> [Accessed 23 Feb. 2016].
- Bakar, N., Chee, C., Abdullah, L., Ratnam, C. and Ibrahim, N. (2015). Thermal and dynamic mechanical properties of grafted kenaf filled poly (vinyl chloride)/ethylene vinyl acetate composites. *Materials & Design (1980-2015)*, 65, pp.204-211.
- Baliga, M., Pai, R., Bhat, H., Palatty, P. and Bloor, R. (2011). Chemistry and medicinal properties of the Bakul (*Mimusops elengi* Linn): A review. *Food Research International*, 44(7), pp.1823-1829.

- BBC, (2014). *Plastics*. [online] Available at: <http://www.bbc.co.uk/schools/gcsebitesize/design/resistantmaterials/materialsmaterialsrev3.shtml> [Accessed 1 Mar. 2016].
- Bjørk, R., Tikare, V., Frandsen, H. and Pryds, N. (2012). The Effect of Particle Size Distributions on the Microstructural Evolution During Sintering. *Journal of the American Ceramic Society*, 96(1), pp.103-110.
- Borkowski, L. (2006). *Greener Paths for Plastics*. [online] Green America. Available at: <http://www.greenamerica.org/livinggreen/plastics.cfm> [Accessed 23 Feb. 2016].
- Boonyuen, C., Wangkarn, S., Suntornwat, O. and Chaisuksant, R. (2009). Antioxidant Capacity and Phenolic Content of Mimusops elengi Fruit Extract. *Kasetsart Journal of Natural Sciences*, 43, pp.21-27.
- Bouza, R., Marco, C., Martin, Z., Gómez, M., Ellis, G. and Barral, L. (2007). Comportamiento de cristalización y fusión en compuestos de polipropileno y derivados de madera. *Revista iberoamericana de polímeros*, 8(1), pp.1-10.
- Colthup, N. (1964). *Introduction to infrared and Raman spectroscopy*. New York: Academic Press.
- Craver, C. and Carraher, C. (2000). *Applied polymer science*. Amsterdam [Netherlands]: Elsevier.
- Das, O., Sarmah, A. and Bhattacharyya, D. (2015). A sustainable and resilient approach through biochar addition in wood polymer composites. *Science of The Total Environment*, 512-513, pp.326-336.
- Das, S. (2009). Jute composite and its applications. *Proceedings of International Workshop IJSG*. [online] Available at: [http://www.jute.org/Documents\\_Seminar\\_Workshop\\_Meeting/Jute%20composite%20and%20its%20Applications\\_S.%20Das\\_IJIRA.doc](http://www.jute.org/Documents_Seminar_Workshop_Meeting/Jute%20composite%20and%20its%20Applications_S.%20Das_IJIRA.doc).
- Deepanraj, A., Gokul, R., Raja, S., Vijayalakshmi, S. and Ranjitha, J. (2015). A Facile Acid-Catalysed Biodiesel Production From The Seeds of Mimusops Elengi. *International Journal of Education and Applied Research*, 10(2), pp.2106-2109.
- Demir, H., Atikler, U., Balköse, D. and Tihminlioğlu, F. (2006). The effect of fiber surface treatments on the tensile and water sorption properties of polypropylene–luffa fiber composites. *Composites Part A: Applied Science and Manufacturing*, 37(3), pp.447-456.
- Dittenber, D. and GangaRao, H. (2012). Critical review of recent publications on use of natural composites in infrastructure. *Composites Part A: Applied Science and Manufacturing*, 43(8), pp.1419-1429.

- D&M Plastic Inc., (2016). *Polypropylene*. [online] D&M Plastic Inc. Available at: <http://www.plasticmoulding.ca/polymers/polypropylene.htm> [Accessed 6 Mar. 2016].
- Dutta, K. and Deka, D. (2014). Physicochemical characteristics and triglyceride composition of Mimusops elengi seed oil. *Advances in Applied Science Research*, 5(1), pp.65-73.
- Dymock, W. (1890). *Pharmacographia indica. A history of the principal drugs of vegetable origin, met with in British India*. London: K. Paul, Trench, Trübner & Co., ld.
- Ensinger, (2016). *Thermoplastics classification*. [online] Available at: <http://www.ensinger-online.com/en/materials/basics-of-plastics/thermoplastics-classification/> [Accessed 1 Mar. 2016].
- Evans, J. (2010). Bioplastics get growing. *Plastics Engineering*, 66(2), pp.14-20.
- Fakhrul, T. and Islam, M. (2013). Degradation Behavior of Natural Fiber Reinforced Polymer Matrix Composites. *Procedia Engineering*, 56, pp.795-800.
- Fan, M., Dai, D. and Huang, B. (2012). Fourier Transform Infrared Spectroscopy for Natural Fibres. In: S. Salih, ed., *Fourier Transform - Materials Nalaysis*, 1st ed. [online] China: InTech, pp.45-68. Available at: <http://www.intechopen.com/books/fourier-transform-materials-analysis/fourier-transform-infraredspectroscopy-for-natural-fibres> [Accessed 15 Aug. 2016].
- Faruk, O., Bledzki, A., Fink, H. and Sain, M. (2012). Biocomposites reinforced with natural fibers: 2000â€“2010. *Progress in Polymer Science*, 37(11), pp.1552-1596.
- Fried, J. (1995). *Polymer science and technology*. Englewood Cliffs, N.J.: Prentice Hall PTR.
- Fu, S., Feng, X., Lauke, B. and Mai, Y. (2008). Effects of particle size, particle/matrix interface adhesion and particle loading on mechanical properties of particulate-polymer composites. *Composites Part B: Engineering*, 39(6), pp.933-961.
- Furness, J. (2013). *Mechanical Properties of Thermoplastics - An Introduction*. [online] AZO Materials. Available at: [http://www.azom.com/article.aspx?ArticleID=510#\\_Deformation](http://www.azom.com/article.aspx?ArticleID=510#_Deformation) [Accessed 4 Mar. 2016].
- Furness, J. (2014). *Thermoplastics - An Introduction*. [online] AZO Materials. Available at: <http://www.azom.com/article.aspx?ArticleID=83> [Accessed 4 Mar. 2016].
- Gao, F. (2004). Clay/polymer composites: the story. *Materials Today*, 7(11), pp.50-55.
- Gourmelon, G. (2015). *Global Plastic Production Rises, Recycling Lags*. [online]

- Worldwatch Institute. Available at: <http://www.worldwatch.org/global-plastic-production-rises-recycling-lags-0> [Accessed 23 Feb. 2016].
- Granda, L., Méndez, J., Espinach, F., Puig, J., Delgado-Aguilar, M. and Mutjé P. (2016). Polypropylene reinforced with semi-chemical fibres of *Leucaena collinsii*: Thermal properties. *Composites Part B: Engineering*, 94, pp.75-81.
- Guan, B., Latif, P. and Yap, T. (2013). Physical Preparation of Activated Carbon From Sugarcane Bagasse And Corn Husk And Its Physical And Chemical Characteristics. *International Journal of Engineering Research and Science & Technology*, 2(3), pp.1-14.
- Hamad, K., Kaseem, M. and Deri, F. (2013). Recycling of waste from polymer materials: An overview of the recent works. *Polymer Degradation and Stability*, 98(12), pp.2801-2812.
- Herz, Y. (2012). *Optimization of Mechanical Properties of Polypropylene-based Composite*. Master. University of Waterloo.
- Hindle, C. (2016). *Polypropylene (PP)*. [online] Bpf.co.uk. Available at: <http://www.bpf.co.uk/plastipedia/polymers/pp.aspx> [Accessed 4 Mar. 2016].
- Intertek. (2016). *Fourier Transform Infrared Spectroscopy (FTIR) Analysis*. [online] Available at: <http://www.intertek.com/analysis/ftir/> [Accessed 17 Jul. 2016].
- Ismail, H. and Mathialagan, M. (2011). Curing Characteristics, Morphological, Tensile and Thermal Properties of Bentonite-Filled Ethylene-Propylene-Diene Monomer (EPDM) Composites. *Polymer-Plastics Technology and Engineering*, 50(14), pp.1421-1428.
- Jacoby, M. (2009). Graphene: Carbon as thin as can be. *Chemical & Engineering News*, 87(9), pp.14-20.
- Jeyasundari, J., Praba, P., Jacob, Y., Rajendran, S. and Kaleeswari, K. (2016). Green Synthesis and Characterization of Silver Nanoparticles Using *Mimusops elengi* Flower Extract and Its Synergistic Antimicrobial Potential. *American Chemical Science Journal*, 12(3), pp.1-11.
- John, M. and Thomas, S. (2008). Biofibres and biocomposites. *Carbohydrate Polymers*, 71(3), pp.343-364.
- Johnson, T. (2014). *What Is Polypropylene Used For?*. [online] About.com Money. Available at: <http://composite.about.com/od/Plastics/a/What-Is-Polypropylene.htm> [Accessed 5 Mar. 2016].
- Joseph, J. and George, M. (2016). Chemical composition and biological activities of the fruit-*Mimusops elengi*. *Journal of Chemical and Pharmaceutical Research*, 8(1),

pp.51-57.

- Kabir, M., Wang, H., Lau, K. and Cardona, F. (2012). Chemical treatments on plant-based natural fibre reinforced polymer composites: An overview. *Composites Part B: Engineering*, 43(7), pp.2883-2892.
- Kadam, P., Yadav, K., Deoda, R., Shivatare, R. and Patil, M. (2012). *Mimusops elengi: A Review on Ethnobotany, Phytochemical and Pharmacological Profile*. *Journal of Pharmacognosy and Phytochemistry*, 1(3), pp.64-74.
- Katz, H. and Milewski, J. (1987). *Handbook of fillers for plastics*. New York: Van Nostrand Reinhold Co.
- Kohls, D. and Beaucage, G. (2002). Rational design of reinforced rubber. *Current Opinion in Solid State and Materials Science*, 6(3), pp.183-194.
- Ku, H., Wang, H., Pattarachaiyakoop, N. and Trada, M. (2011). A review on the tensile properties of natural fiber reinforced polymer composites. *Composites Part B: Engineering*, 42(4), pp.856-873.
- Kuruppallil, Z. (2011). Green Plastics: An Emerging Alternative for Petroleum Based Plastics?. *International Journal of Engineering Research & Innovation*, 3(1), pp.59-64.
- Lalithamba, (2011). *Mimusops elengi Images*. [online] Useful Tropical Plants Database. Available at: <http://tropical.theferns.info/image.php?id=Mimusops+elengi> [Accessed 8 Aug. 2016].
- Lu, X. and Xu, G. (1997). Thermally conductive polymer composites for electronic packaging. *Journal of Applied Polymer Science*, 65(13), pp.2733-2738.
- Mark, H. (2007). *Encyclopedia of polymer science & technology, concise*. Hoboken, N.J.: J. Wiley.
- Mark, J. (2006). *Physical properties of polymer handbook*. New York: Springer.
- Matějka, V., Fu, Z., Kukutschová, J., Qi, S., Jiang, S., Zhang, X., Yun, R., Vaculík, M., Heliová M. and Lu, Y. (2013). Jute fibers and powderized hazelnut shells as natural fillers in non-asbestos organic non-metallic friction composites. *Materials & Design*, 51, pp.847-853.
- Miguez Suarez, J., Coutinho, F. and Sydenstricker, T. (2003). SEM studies of tensile fracture surfaces of polypropylene—sawdust composites. *Polymer Testing*, 22(7), pp.819-824.
- Mitra, R. (1981). Bakula-A reputed drug of Ayurveda, its history, uses in Indian medicine. *Indian Journal of History of Science*, 16(2), pp.169-180.



- Mohammed, L., Ansari, M., Pua, G., Jawaid, M. and Islam, M. (2015). A Review on Natural Fiber Reinforced Polymer Composite and Its Applications. *International Journal of Polymer Science*, 2015, pp.1-15.
- Mohanty, A., Misra, M. and Drzal, L. (2005). *Natural Fibers, Biopolymers, and Their Biocomposites*. London: CRC Press.
- Muniandy, K., Ismail, H. and Othman, N. (2012). Biodegradation, Morphological and FTIR Study of Rattan Powder-Filled Natural Rubber Composites as A Function of Filler Loading And A Silane Coupling Agent. *BioResources*, 7(1), pp.957-971.
- Mwaikambo, L. and Ansell, M. (2002). Chemical modification of hemp, sisal, jute, and kapok fibers by alkalization. *Journal of Applied Polymer Science*, 84(12), pp.2222-2234.
- NDT Resource Center, (2016). *Polymer Structure*. [online] Available at: <https://www.nde-ed.org/EducationResources/CommunityCollege/Materials/Structure/polymer.htm> [Accessed 1 Mar. 2016].
- North, E. and Halden, R. (2013). Plastics and environmental health: the road ahead. *Reviews on Environmental Health*, 28(1), pp.1-8.
- Nurshamila, S., Ismail, H. and Othman, N. (2012). The Effects of Rattan Filler Loadings on Properties of Rattan Powder-Filled Polypropylene Composites. *BioResources*, 7(4).
- OpenLearn, (2011). *Introduction to polymers*. [online] Available at: <http://www.open.edu/openlearn/science-maths-technology/science/chemistry/introduction-polymers/content-section-1.2.2> [Accessed 29 Feb. 2016].
- Pang, A., Ismail, H. and Abu Bakar, A. (2015). Effects of Kenaf Loading on Processability and Properties of Linear Low-Density Polyethylene/Poly (Vinyl Alcohol)/Kenaf Composites. *BioResources*, 10(4).
- Paroli, R., Liu, K. and Simmons, T. (1999). *Schematic molecular configurations of (a) a thermoplastic and (b) a thermoset*. [image] Available at: [http://www.nrc-nrc.gc.ca/ctu-sc/ctu\\_sc\\_n30](http://www.nrc-nrc.gc.ca/ctu-sc/ctu_sc_n30) [Accessed 1 Mar. 2016].
- Pickering, K. (2008). *Properties and performance of natural-fibre composites*. Boca Raton: CRC Press.
- Pollutionissues.com, (2008). *Plastic*. [online] Available at: <http://www.pollutionissues.com/Pl-Re/Plastic.html> [Accessed 19 Feb. 2016].
- Polymer Resources, LTD. (2013). *Amorphous Thermoplastics - Characteristics of Non-crystalline materials*. [online] Available at: <http://www.prlresins.com/custom->

engineered-plastic-resins-blog/item/6-amorphous-thermoplastics-characteristics-of-non-crystalline-materials [Accessed 5 Aug. 2016].

Pritchard, G. (2007). Plants move up the reinforcement agenda. *Plastics, Additives and Compounding*, 9(4), pp.40-43.

Prnewswire.com, (2015). *Global Polymer Industry 2015-2020: Trend, Profit, and Forecast Analysis*. [online] Available at: <http://www.prnewswire.com/news-releases/global-polymer-industry-2015-2020-trend-profit-and-forecast-analysis-300131254.html> [Accessed 19 Feb. 2016].

Pujari, S., Ramakrishna, A. and Kumar, M. (2014). Comparison of Jute and Banana Fiber Composites: A Review. *International Journal of Current Engineering and Technology*, 2(2), pp.121-126.

Ragunathan, K. and Mitra, R. (2000). Pharmacognosy of Indigenous Drugs. *Government of India: Central council for Research in Ayurveda and Siddha*, 1, pp.158-183.

Rajkumara, S., Pandiselvi, A. and Sandhiya, G. (2012). Isolation of Chemical Constituents from *Mimusops elengi* bark and Evaluation of Anti-inflammatory activity. *International Journal Phytopharmacy*, 3(1), pp.9-15.

Rashid, M. (2010). *Comparative advantages of Jute to be used for shopping bag*. [online] Bangladesh Textile Today. Available at: <http://www.textiletoday.com.bd/comparative-advantages-of-jute-to-be-used-for-shopping-bag/> [Accessed 4 Mar. 2016].

Redwood Plastics, (2016). *Amorphous vs. Semi-Crystalline Thermoplastics*. [online] Redwood Plastics. Available at: <https://www.redwoodplastics.com/education-2/amorphous-vs-semi-crystalline-thermoplastics/> [Accessed 4 Mar. 2016].

Remichem OÜ, (2016). *Polyethylene*. [online] Remichem OÜ. Available at: <http://www.remichem.com/polyethylene.html> [Accessed 6 Mar. 2016].

Riley, A., Paynter, C., McGenity, P. and Adams, J. (1990). Factors affecting the impact properties of mineral-filled polypropylene. *lastics and Rubber Processing and Applications*, 14(2), pp.85-93.

Roqaiya, M., Begum, W., Majeedi, S. and Saiyed, A. (2015). A review on traditional uses and phytochemical properties of *Mimusops elengi* Linn. *International Journal of Herbal Medicine*, 2(6), pp.20-23.

Rothon, R. (2002). *Particulate fillers for polymers*. Shawbury, U.K.: Rapra Technology Ltd.

RTP Company, (2015). *Semi-Crystalline Polymers*. [online] RTP Company. Available at: <http://www.rtpcompany.com/products/high-temperature/semi-crystalline-polymers/> [Accessed 4 Mar. 2016].

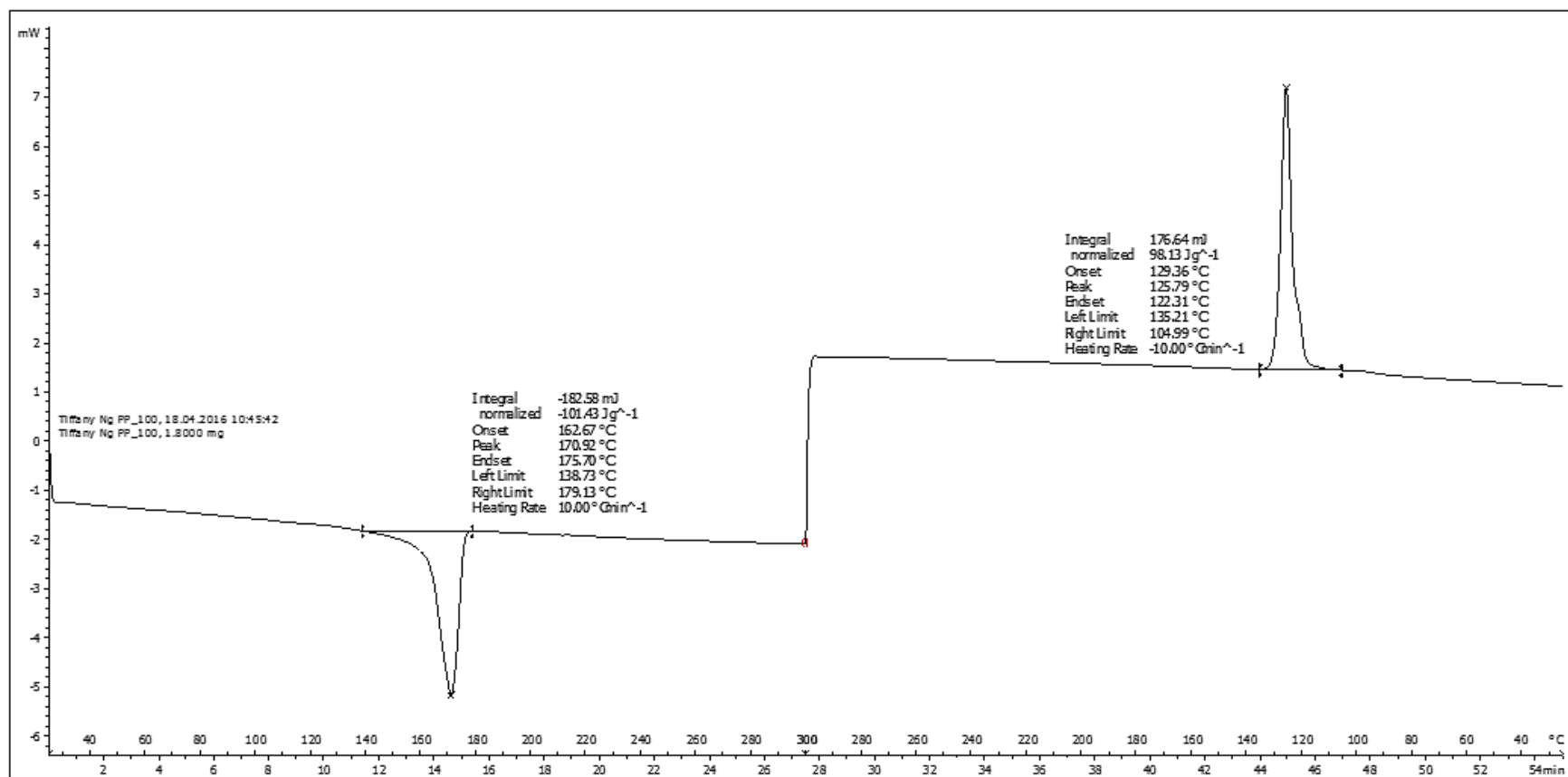
- Science.jrank.org, (2016). *Plastics - Thermoplastics*. [online] Available at: <http://science.jrank.org/pages/5318/Plastics-Thermoplastics.html> [Accessed 29 Feb. 2016].
- Shao, X., He, L. and Ma, L. (2015). Water Absorption and FTIR Analysis of Three Type Natural Fiber Reinforced Composites. *International Forum on Electrical Engineering and Automation*, pp.269-272.
- Shibata, S., Cao, Y. and Fukumoto, I. (2006). Lightweight laminate composites made from kenaf and polypropylene fibres. *Polymer Testing*, 25(2), pp.142-148.
- Shimadzu Corporation. (2016). *Particle Size Distribution Dependent on Principle of Measurement : SHIMADZU (Shimadzu Corporation)*. [online] Available at: <http://www.shimadzu.com/an/powder/support/practice/p01/lesson02.html> [Accessed 18 Mar. 2016].
- Silva, E., Ribeiro, L., Nascimento, M. and Ito, E. (2014). Rheological and mechanical characterization of poly (methyl methacrylate)/silica (PMMA/SiO<sub>2</sub>) composites. *Mat. Res.*, 17(4), pp.926-932.
- Stuart, B. (2004). *Infrared spectroscopy*. Chichester, Eng.: J. Wiley.
- Textile Technologist, (2012). *Polypropylene Fiber | Physical And Chemical Properties Of Polypropylene | Textile Fashion Study*. [online] Textile Fashion Study. Available at: <http://textilefashionstudy.com/polypropylene-fiber-physical-and-chemical-properties-of-polypropylene/> [Accessed 6 Mar. 2016].
- Thomas, S. and Pothan, L. (2009). *Natural fibre reinforced polymer composites*. Paris: Éd. des Archives contemporaines.
- Tisserat, B., Reifschneider, L., Carlos López Núñez, J., Hughes, S., Selling, G. and Finkenstadt, V. (2014). Evaluation of the Mechanical and Thermal Properties of Coffee Tree Wood Flour - Polypropylene Composites. *BioResources*, 9(3).
- Toyota Boshoku. (2016). *Kenaf*. [online] Available at: <http://www.toyota-boshoku.com/global/about/development/eco/kenaf/> [Accessed 14 Mar. 2016].
- Tver, D. and Bolz, R. (1984). *Encyclopedic dictionary of industrial technology*. New York: Chapman and Hall.
- University of York, (2014). *Poly(propene) (Polypropylene)*. [online] CIEC Promoting Science. Available at: <http://www.essentialchemicalindustry.org/polymers/polypropene.html> [Accessed 5 Mar. 2016].
- Viet, C., Ismail, H., Rashid, A. and Takeichi, T. (2012). Kenaf Powder Filled Recycled High Density Polyethylene/ Natural Rubber Biocomposites: The Effect of Filler

- Content. *International Journal of Integrated Engineering*, 4(1), pp.22-25.
- Wong, K., Yousif, B. and Low, K. (2010). The effects of alkali treatment on the interfacial adhesion of bamboo fibres. *Proceedings of the Institution of Mechanical Engineers, Part L: Journal of Materials Design and Applications*, 224(3), pp.139-148.
- Wypych, G. (1999). *Handbook of fillers*. Toronto, Ont.: ChemTec.
- Xanthos, M. (2010). *Functional fillers for plastics*. Weinheim: Wiley-VCH.
- Xanthos, M. and Todd, D. (1996). Plastics processing. In: *Kirk-Othmer Encyclopedia of Chemical Technology*, 4th ed. New York: John Wiley&Sons, Inc., pp.290-316.
- Zakaria, S. and Kok Poh, L. (2002). Polystyrene-benzoylated EFB reinforced composites. *Polymer-Plastics Technology and Engineering*, 41(5), pp.951-962.
- Zou, Y., Feng, Y., Wang, L. and Liu, X. (2004). Processing and properties of MWNT/HDPE composites. *Carbon*, 42(2), pp.271-277.

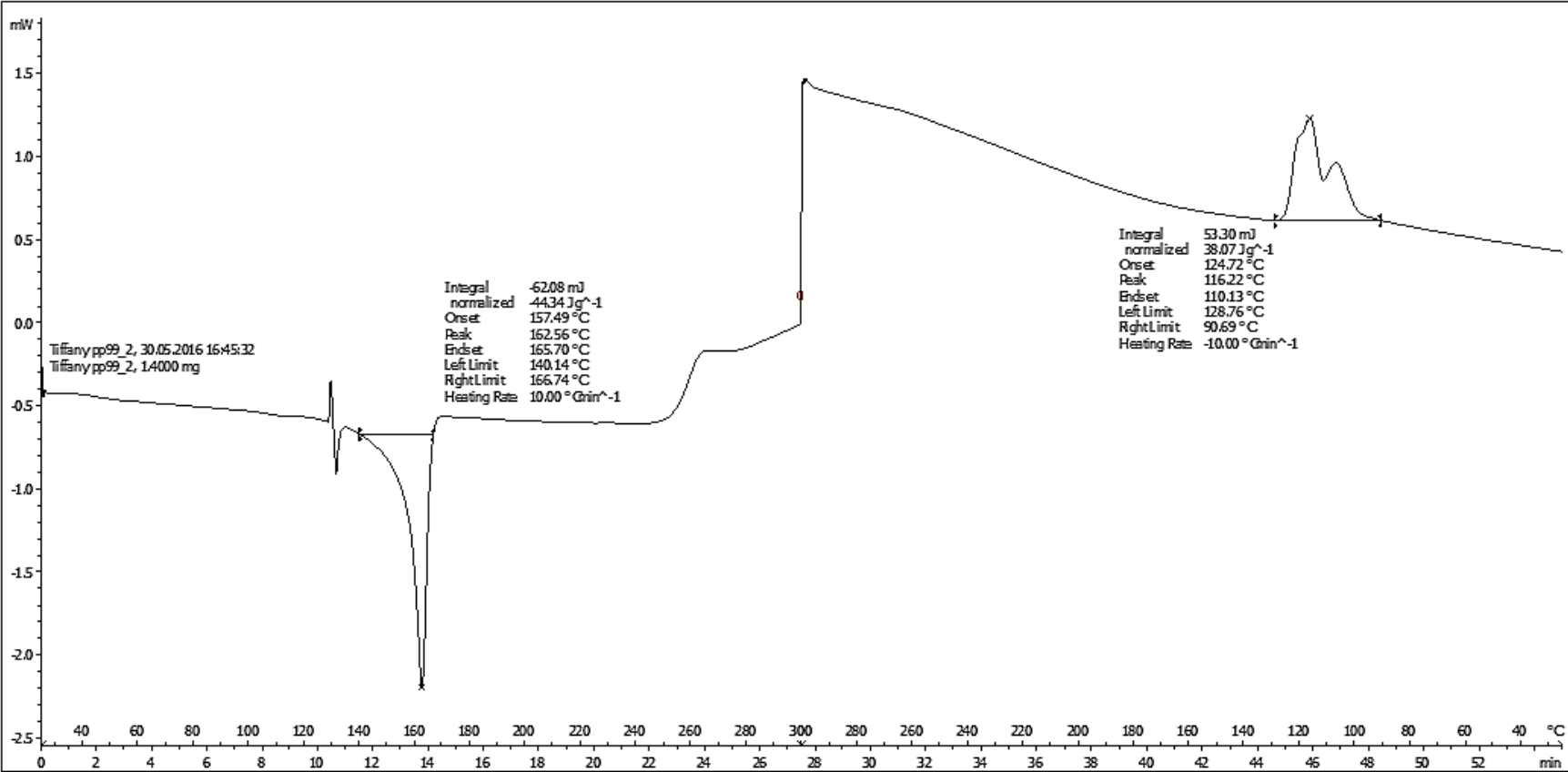
## **APPENDICES**

### APPENDIX A: Differential Scanning Calorimetry

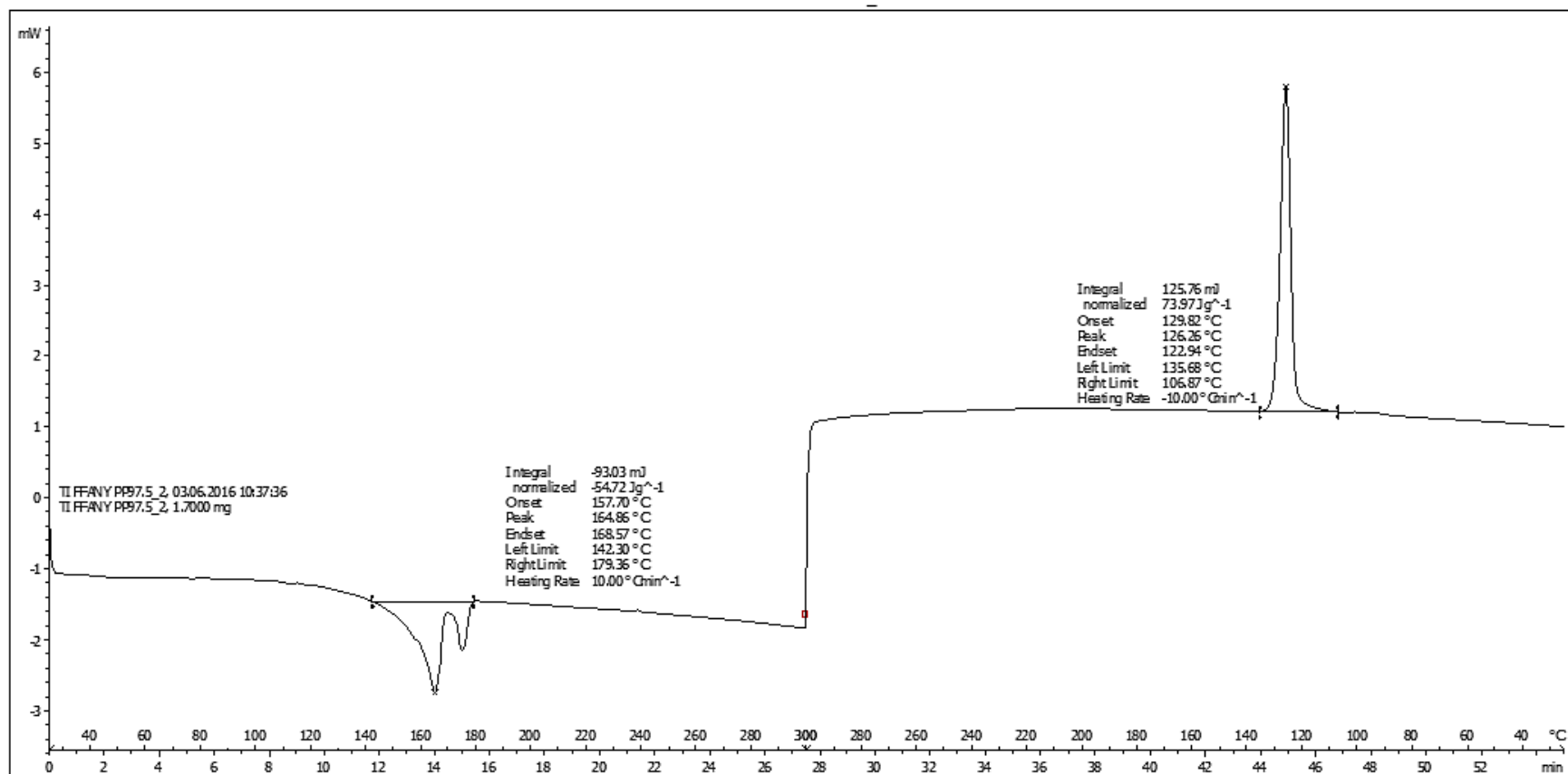
## (a) Unfilled PP



(b) PP / 1 wt% MESSP

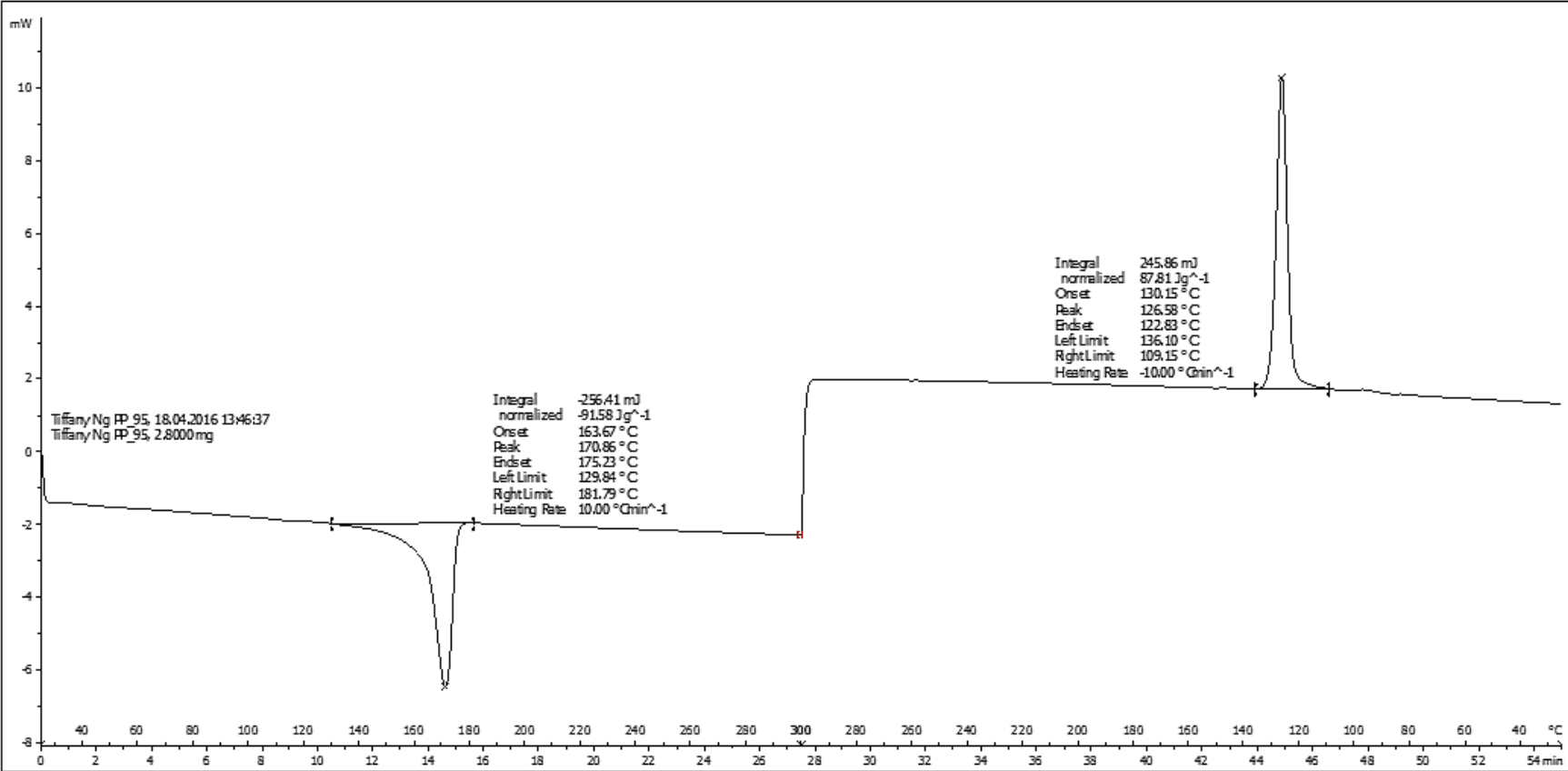


(c) PP/ 2.5 wt% MESSP

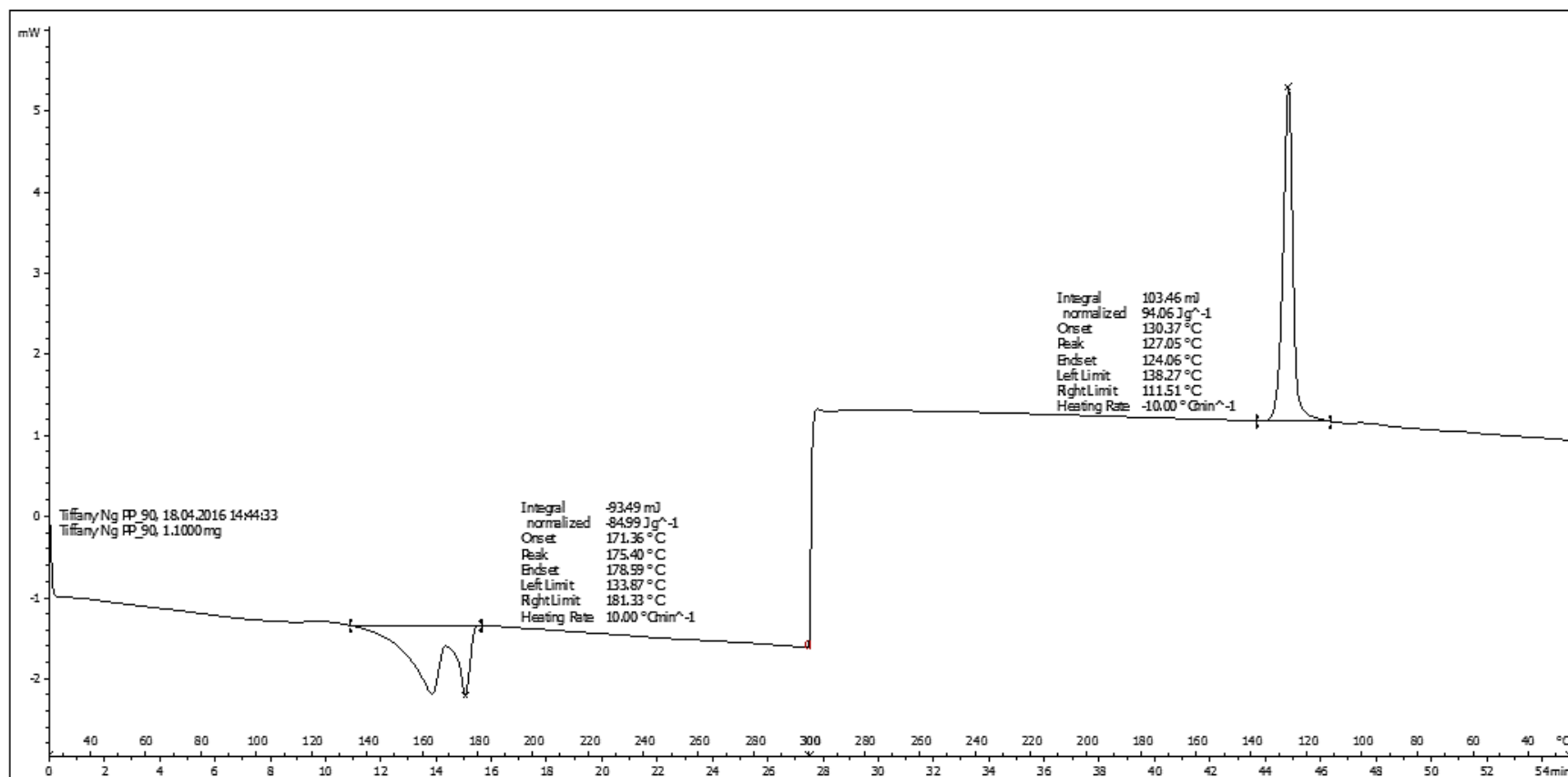




(d) PP / 5 wt% MESSP

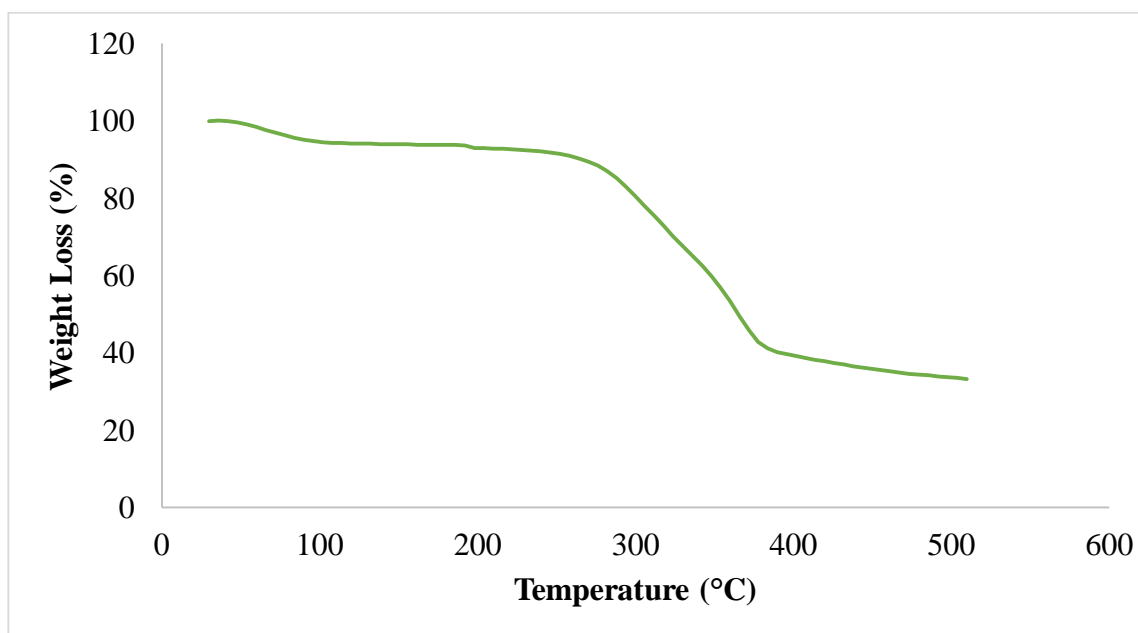


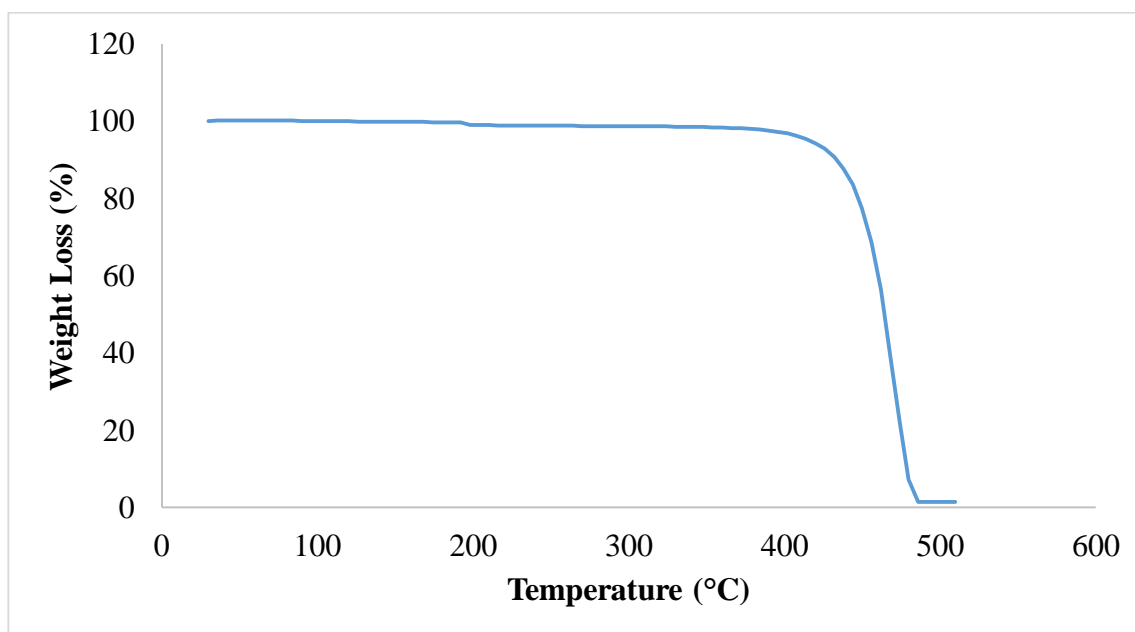
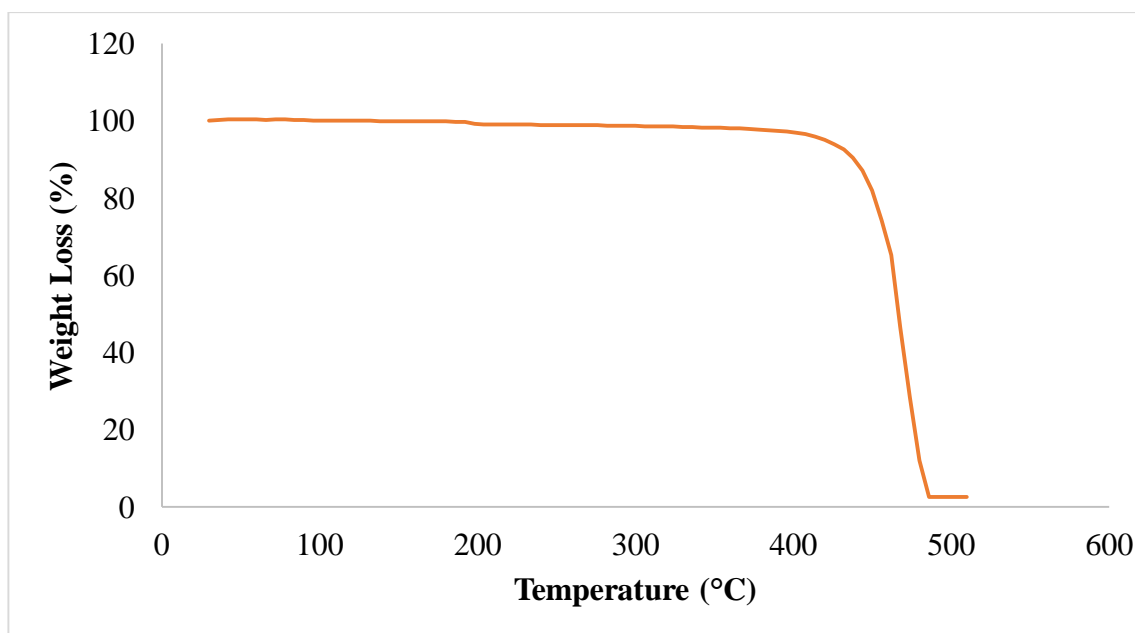
## (e) PP / 10 wt% MESSP

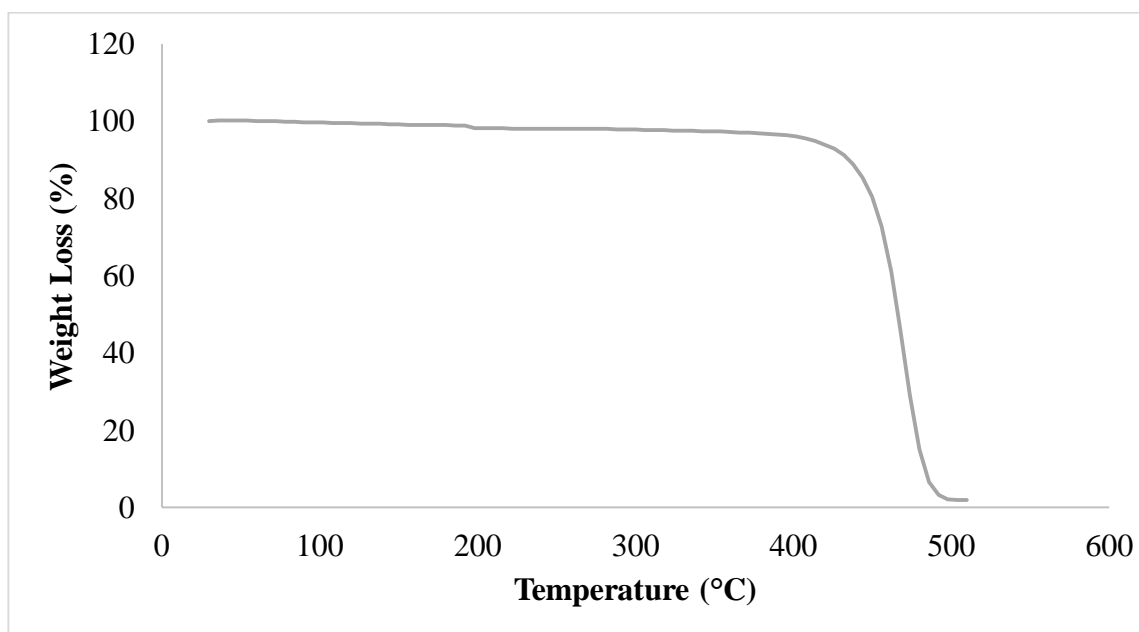
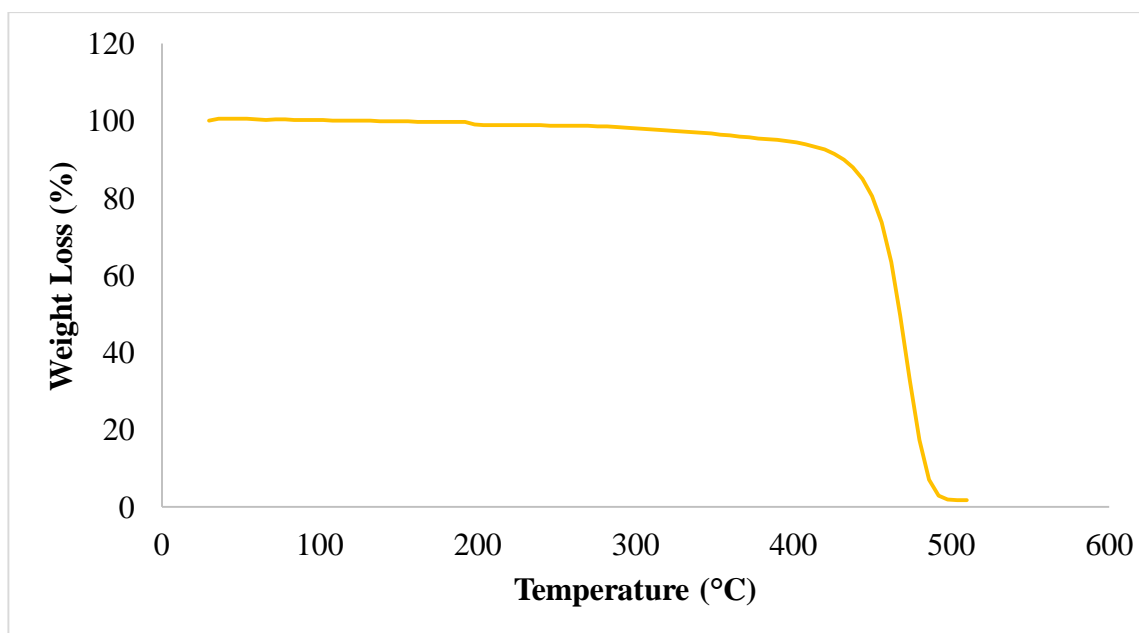


## APPENDIX B: Thermogravimetric Analysis

(a) Raw MESSP



**(b) Unfilled PP****(c) PP / 1 wt% MESSP**

**(d) PP / 2.5wt% MESSP****(e) PP / 5 wt% MESSP**

**(f) PP / 10 wt% MESSP**